



Universidad de Valladolid

Facultad de Ciencias

TRABAJO FIN DE GRADO

Grado en Química

Molecular Modelling and Rotational Spectroscopy of Multiconformational Systems

Autor: Elena Caballero Mancebo

Tutor: Alberto Lesarri Gómez

Index:

1. Abstract.....	1
1.1 Abstract of the project.....	1
1.2 Resumen del proyecto.....	1
2. Introduction	3
2.1 General anesthetics and structural analysis.....	3
2.2 Objectives	7
3. Methodology.....	9
3.1 Rotational spectroscopy	10
3.1.1 Rotational Hamiltonian.....	10
3.1.2 Selection Rules.....	13
3.1.3 Centrifugal distortion.....	15
3.1.4 Nuclear quadrupole coupling	16
3.2 Computational Methods.....	18
3.2.1 Molecular Mechanics.....	18
3.2.2 Conformational search	20
3.2.3 Semiempirical methods	21
3.2.4 Ab initio and Density-Functional Theory:.....	21



4. Results.....	25
4.1 Computational modelling	25
4.1.1 Conformational search	26
4.1.2 Density-Functional-Theory and ab initio calculations	27
4.2 Spectral analysis.....	36
4.2.1 Conformer A	36
4.2.2 Conformer B.....	41
4.2.3 Conformer C.....	46
4.2.4 Isotopic species.....	47
4.2.5 Conformational assignment	51
4.2.6 Structural determination	54
5. Conclusions	59
6. References	63
7. Annexes	67



1. Abstract

1.1 Abstract of the project

The Project presented here is a spectroscopic, computational and structural study of the molecule enflurane. This molecule has been used as general anesthetic, and illustrates the advantages of using rotational spectroscopy to investigate the structural properties of molecules with multiple conformational possibilities. This study includes both computational and spectroscopic results. An extensive conformational search was conducted using molecular mechanics, and all the species were re-examined using ab initio and density-functional theory calculations. The rotational spectrum has been analysed using experimental data in the region 2-18 GHz. Three conformations have been detected in the gas-phase and their rotational, centrifugal distortion and nuclear quadrupole coupling parameters have been determined. The analysis was extended to several isotopic species innatural abundance (^{35}Cl , ^{37}Cl and the three ^{13}C species of the most intense conformer). Finally, the rotational data allowed determining the molecular structure of the most stable conformation. The preferred conformations of enflurane share a common C-C-O-C *trans* skeleton, with the chlorine atoms either in *gauche* (G^- , G^+) or *trans* (T) orientations.

1.2 Resumen del proyecto

El proyecto presente es un estudio espectroscópico, computacional y estructural de la molécula de enflurano. Esta molécula se ha empleado como anestésico general, e ilustra las ventajas del uso de la espectroscopía de rotación para la investigación de propiedades estructurales de moléculas con múltiples posibilidades conformacionales. Este estudio incluye resultados tanto computacionales como espectroscópicos. Se ha llevado a cabo una búsqueda conformacional exhaustiva empleando mecánica molecular, y todas las especies se han reexaminado empleando cálculos ab initio y teoría del funcional de la densidad. El espectro de rotación se ha analizado utilizando datos experimentales en la región 2-18 GHz.



Se han detectado tres conformaciones en fase gas, y se han determinado las constantes de rotación y los parámetros de distorsión centrífuga y acoplamiento de cuadrupolo nuclear. El análisis se ha extendido a varias especies isotópicas en abundancia natural (^{35}Cl , ^{37}Cl y las tres especies ^{13}C del conformero más intenso). Finalmente, los datos de rotación han permitido determinar la estructura de la molécula en la conformación más estable. Las conformaciones más estables de enflurano comparten un esqueleto C-C-O-C *trans*, con el átomo de cloro en orientación *gauche* (G-, G+) o *trans* (T).



2. Introduction

2.1 General anesthetics and structural analysis

This work describes a spectroscopic, computational and structural study of the molecule 2-chloro-1,1,2-trifluoroethyl-difluoromethyl ether (enflurane), a general volatile anesthetic mostly used clinically in the 1970's and 1980's.

Anesthetics are drugs used in surgery that cause loss of sensation during medical operations. A wide variety of drugs is used in modern anesthetic practice. These chemical compounds can have their effects limited to a particular region in the body maintaining the consciousness of the subject (*local anesthetics*), or they may have general effects causing reversible loss of consciousness (*general anesthetics*).

The general anaesthetics are a structurally diverse group of compounds (monoatomics, diatomics, ethers, phenols, etc) whose mechanisms encompass multiple biological targets involved in the control of neuronal pathways. The exact effects that general anesthetics produce in the human body are not totally determined, but the accepted hypothesis is that anesthetics bind to the proteins of the ionic channels involved in the neuronal synapsis, inhibiting the nervous signals [1].

For these reasons the study and determination of different families of anesthetic structures is needed in order to eventually understand the molecular interactions which determine their biological functions.

Condensed phase studies have the advantage that they can simulate or reproduce the biological environment where drugs are applied. For example, there are some crystal diffraction studies of anesthetics bound to soluble proteins, which can help to identify the binding sites during anesthetic action [2]. However, molecular properties and intermolecular interactions can get masked by interaction with a solvent or crystal, so the factors controlling a chemical compound would not be clear. Alternatively, gas phase studies allow



us to determine accurate molecular structures and to distinguish the intrinsic molecular properties from those imposed by the solvent or crystal [3].

In consequence, gas phase studies represent a remote situation from the biological environment, but they generate very important information about these molecules and their interactions. Among the different spectroscopic techniques, microwave spectroscopy is the method of choice for the accurate determination of molecular structures, since it offers very high resolution (kHz) and can analyze separately all possible species in the gas phase, like isomers or isotopologues [4]. In recent years most microwave experiments are conducted in supersonic jets, which additionally offer much smaller linewidths, a cooled ($T \sim 2$ K) and collision-free environment and the possibility of generation of intermolecular clusters [5]. In this work, we analyzed the supersonic jet spectrum of enflurane in the region 2-18 GHz. The results can be directly compared with theoretical ab initio calculations, which represent the molecule in isolation conditions. The combination of experimental and theoretical data represents a powerful approach to the investigation of molecular structures and at the same time a benchmark for the theoretical models. In this work we have combined several ab initio and DFT calculations and compared the result with the experimental data.

Enflurane is a volatile liquid used as inhaling anesthetic. It belongs to a family of fluorinated compounds that was discovered during the 1950s, when three compounds with these characteristics were introduced into clinical practice: fluoroxene ($\text{CF}_3\text{CH}_2\text{OCH}=\text{CH}_2$) by Ohio Medical Products in 1951, halothane (CF_3CHClBr) by Ayerst Laboratories and Imperial Chemical Industries in 1955, and methoxyflurane ($\text{CH}_3\text{OCF}_2\text{CHCl}_2$) by Abbott Laboratories in 1959. Although several other fluorinated ethers were reported to have anesthetic properties, none were successfully marketed. Some of these drugs produced clinical problems, so over the next 10 or 15 years hundreds of new fluorinated compounds were synthesized, four of which – enflurane ($\text{CHF}_2\text{OCF}_2\text{CHFCl}$), isoflurane ($\text{CF}_3\text{CFHClOCHF}_2$), sevoflurane ($(\text{CF}_3)_2\text{CHOCH}_2\text{F}$) and desflurane ($\text{CF}_3\text{CHFOCHF}_2$) – are still currently used in clinical practice [6].

Our group has recently studied the structural properties of sevoflurane [7] and isoflurane [8] combining rotational spectroscopy and ab initio data. Desflurane was also investigated by the group of Brooks Pate in Virginia using the same methodology [9]. However, two more compounds, enflurane and methoxyflurane have not been reported yet, despite some preliminary results were available in our group. In this work we have completed the analysis of enflurane with the observation of two more isomers and several isotopologues. The results permit now to present a global view of the conformational and structural properties of the molecule.

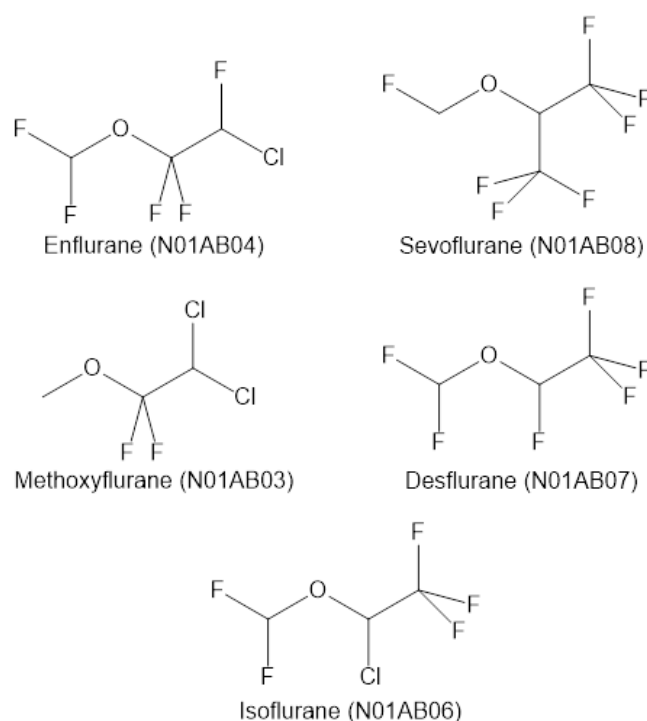


Figure 2.1. Halogenated ethers used as volatile anesthetics (World Health Organization NTC codes in parentheses).

There was some previous information on enflurane in the bibliography. Oberhammer *et al.* studied enflurane in 1998 using gas-electron diffraction (GED) [10]. He concluded that the gas phase was populated by three conformations (all with a *trans* C-C-O-C skeleton) with relative populations of 58%, 32% and 10%. According to his investigation the most populated



conformer has the Cl-C bond *trans* to the central C-O bond. However, this technique cannot resolve conformers which have similar structures and the GED conclusions may not be univocal in complex molecules with several coexisting conformers. For these reasons, these authors concluded that “*the enflurane problem is really underdetermined experimentally*”. Oberhammer also conducted ab initio calculations (HF, B3PW91, MP2) and a conformational search to complement the experimental data, which resulted in nineteen different structures. Considering that the interpretation of diffraction data may be complicated in case of multiple conformations, it might be possible that this structural analysis has been biased by the theoretical predictions and would require further investigation.

The previous conclusions on a *trans* C-C-O-C skeleton were supported by DFT (B3LYP), natural-bond-orbital (NBO) analysis and low-resolution (1 cm^{-1}) infrared data in CCl_4 and low-temperature cryogenic matrix obtained by Zeegers-Huyskens *et al.* These authors claimed to have observed four conformers in the IR spectrum [11], but this result was mostly based in the conclusions of the GED work. Another vibrational circular dichroism (VCD) study complemented by DFT calculations (B3LYP) examined the low-resolution (4 cm^{-1}) IR spectrum in CS_2 , similarly proposing that enflurane was composed of four conformations in solution [12]. The interpretation of IR data should be probably considered with caution because it is also difficult to resolve close conformations in the vibrational spectrum. Additionally, the conditions in condensed phases cannot be compared directly with the gas phase.

Information from NMR spectroscopy was also available, but it concluded that the C-C-O-C skeleton was not planar [13], opposing the experimental results of GED and IR spectra.

There are also some studies (mostly theoretical) on enflurane clusters, in particular with water [14], acetone [15], formaldehyde [16] and benzene [17]. All these studies examine the different intermolecular interactions of enflurane, so they would benefit from a detailed understanding of the structural properties of the molecule.



2.2 Objectives

The objectives of this work are:

- To carry out an extended conformational search and ab initio and density-functional theoretical predictions, to establish the conformational composition and relative energies of the most stable isomers of enflurane.
- To analyze all the experimental spectra obtained by microwave spectroscopy of enflurane to date, in order to assign all possible species in the gas phase and to determine their rotational constants, centrifugal distortion terms and hyperfine parameters.
- To detect the presence in the microwave spectrum of low-abundance isotopologues (^{13}C , ^{18}O) to obtain inertial information on isotopic species.
- To determine an accurate experimental structure of enflurane using the rotational data to evaluate the theoretical predictions.
- To solve the conformational uncertainties of previous GED, NMR and IR works, providing a definitive and comprehensive structural description of enflurane.



3. Methodology

We present in this chapter the spectroscopic and theoretical methodologies used in our work. Because most of these methods are well known we present a short and general description, emphasizing only those that have been used in our work. A complete description of the spectroscopic and theoretical methods can be found in the bibliography [18,19,20,21].

Structural Chemistry deals with molecules and aggregates. Understanding molecules requires a detailed description of their electronic distribution, vibrational properties and structure, usually demanding multiple pieces of information, both experimental and theoretical. Molecules interact and react, so we need to know not only the intramolecular factors defining the structure, but also which are the most important intermolecular forces controlling aggregation properties.

In consequence, the combination of theoretical and experimental results is the most powerful method to obtain a detailed description of the molecular properties and the best approach to improve our knowledge on the intramolecular factors which determine the molecular structure, like orbital effects or intramolecular hydrogen bonding.

In particular, the combination of molecular orbital calculations and rotational spectroscopy produces very accurate structural information and is the method of choice for relatively small molecules (< aprox. 50 atoms) in the gas phase. For this reason, we present first the most important aspects concerning the analysis of rotational spectra (section 3.1). The 3.2 section describes the theoretical methods.



3.1 Rotational spectroscopy

3.1.1 Rotational Hamiltonian

Rotational Spectroscopy is based on the measurement of the molecular transitions between quantized rotational levels, which usually appear in the microwave region (cm-, mm- or sub-mmw wavelengths, frequencies < 1 THz). From these transitions, information about molecular properties like intramolecular dynamics or structure can be obtained [4]. Rotational spectroscopy is a method of choice for polar molecules in the gas phase and is applied both for laboratory measurements or radiotelescope observations from space. Several textbooks on this technique are available [18-20].

The discussion of the rotational spectra starts with a consideration of the rotational Hamiltonian. Initially, we use the rigid-rotor approximation to derive expressions of the classical Hamiltonian, from which the quantum mechanical Hamiltonian can be derived using well known methods.

Both classical and quantum mechanical Hamiltonians depend on the molecular moments of inertia. Usually the molecular reference system is set-up in the principal-inertial-axes system (PAS, with axes denoted a , b , c), in which the tensor of inertia is diagonal. Conventionally the three principal moments of inertia are defined such that $I_a < I_b < I_c$. Since the rotational Hamiltonian depends on the moments of inertia there are different expressions depending of the molecular symmetry. Molecules can be classified in terms of their values of its moment of inertia as follows:

- Linear molecules: $I_a = 0 < I_b = I_c$
- Spherical tops: $I_a = I_b = I_c$
- Symmetric tops: Prolate: $I_a < I_b = I_c$
Oblate: $I_a = I_b < I_c$
- Asymmetric top: $I_a < I_b < I_c$



For linear and top symmetric molecules the rotational Hamiltonian can be expressed in analytical forms and the calculation of the energy levels is straightforward. However, most of the chemically important molecules are asymmetric tops, for which there are no explicit expressions except for the low quantum levels and the spectrum can be very complex and difficult to analyze. The presence of additional fine or hyperfine interactions, like large-amplitude motions or electric and magnetic interactions may add additional complexity to the spectra.

We will summarize here the most relevant aspects of the treatment of asymmetric rotors. A detailed description is found in the bibliography [18-20].

The rotational energy levels of a linear top are quantized in terms of the total angular momentum quantum number (usually denoted $J = 0, 1, \dots$). These levels are usually degenerate in the projection of the angular momentum on the space-fixed axes (quantum number M). In symmetric tops an additional quantum number appears, accounting for the projection of the angular momentum on the internal symmetry axis ($K = 0, 1, \dots, |J|$, or $J+1$ degeneracy). However, in asymmetric rotors there is no internal component of the angular momentum which is a constant of motion, so this projection does not commute with the Hamiltonian. In consequence, K is not a good quantum number and cannot be used. Alternatively, the rotational energy levels are labeled with two pseudo-quantum numbers (K_a and K_c or K_{-1} and K_{+1}), which correspond to the limiting cases of symmetric prolate and oblate molecules. Rotational energy levels are thus designated with the quantum numbers $J(K_a, K_c)$ (alternatively J_τ , with $\tau = K_a - K_c$). The energy levels can be classified according to the symmetry of the rotational Hamiltonian (point group D_2 or V), given implicitly in the parity of the limiting indices.

The notation of the rotational energy levels is usually explained in the correlation diagram of Figure 3.1, showing as limiting cases the rotational levels of the prolate and oblate symmetric tops. In the left side of the correlation diagram we have the prolate limit, with the rotational energy increasing with J and K . In the right side we have the oblate limit, in which the rotational energy decreases with K . The center of the diagram represents the situation of an asymmetric top, in which all K levels (except $K=0$), previously degenerate for the symmetric rotor, are split into $+K$ and $-K$ values ($2J+1$ degeneracy). The approximate

ordering of the asymmetric rotor levels can then be obtained joining the levels of the limit prolate and oblate cases.

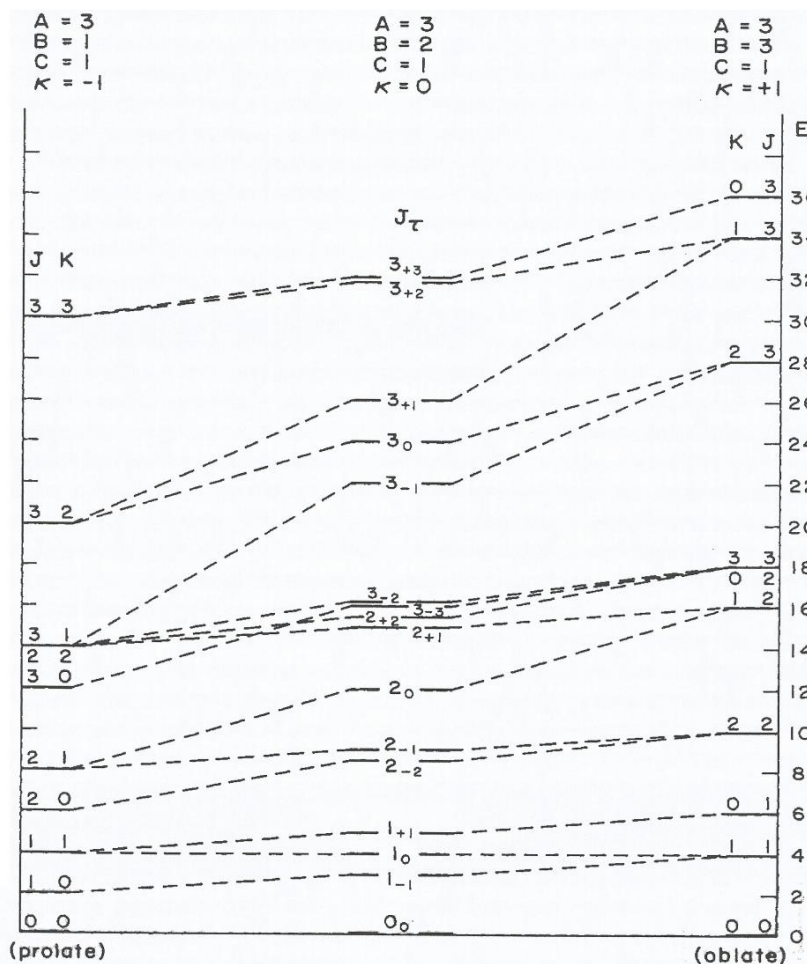


Figure 3.1. Correlation of the rotational energy levels of an asymmetric rotor (center) with those of the limiting cases of a prolate (left) or oblate (right) symmetric top, respectively.

The asymmetric character can be evaluated using the Ray's parameter:

$$\kappa = \frac{2B - A - C}{A - C}$$

which can take any value from -1 to +1, corresponding to the prolate and oblate top limits, respectively. The most asymmetric situation would correspond to $\kappa = 0$. When an asymmetric molecule tends to the prolate ($I_b \rightarrow I_c$) or oblate ($I_b \rightarrow I_a$) limit the rotational spectrum has some characteristics resembling those of the symmetric tops.



The molecular rotational Hamiltonian can be expressed in terms of three parameters called rotational constants (A , B , C), defined as

$$A = \frac{h^2}{8\pi^2 I_a} \quad B = \frac{h^2}{8\pi^2 I_b} \quad C = \frac{h^2}{8\pi^2 I_c}$$

The general expression is then

$$\mathbf{H}_{rot} = A \mathbf{J}_a^2 + B \mathbf{J}_b^2 + C \mathbf{J}_c^2$$

The Schrödinger equation cannot be solved for an asymmetric rotor, so the problem is solved using diagonalization for each J value. A general expression for the wave functions is also not possible, but these functions can be represented as linear combination of the functions of a symmetric top:

$$\Psi_{J,M} = \sum_{J,K,M} a_{JKM} \Psi_{JKM}$$

with a_{JKM} being a numerical constants and Ψ_{JKM} the wave functions of the symmetric rotor. There are many computer programs for the calculation of the rotational energy levels and for the fitting of the observed spectra. In this work we used the CALPGM suite written by Pickett [22], which is freely available from the JPL [23].

3.1.2 Selection Rules

The allowed changes in the angular momentum quantum number (J) for an electric-dipole transition are:

$$\Delta J = 0, \pm 1$$

These allowed transitions result from the non-zero property of the elements in the transition moment matrix: $\int A_{J\tau} \cdot \mu \cdot A_{J'\tau'} \cdot d\tau$. For J' values different from $J'=J''$ or $J'=J''\pm 1$, all the elements in the transition moment will be zero along the three inertial axes. This would be an expected result, because the wave functions of the asymmetric rotor are expressed as a linear combination of the wave functions of the symmetric rotor, which have



the same selection rules. The transitions associated with the selection rules $\Delta J = -1, 0$ and $+1$ are denoted as *P*-, *Q*- or *R*- branch.

The selection rules corresponding to the pseudo-quantum numbers K_a and K_c can be obtained from the symmetry properties of the inertial ellipsoid and can be expressed in terms of the parity of the quantum levels (e: even, o: odd). Three different permitted transitions can be distinguished, depending of component of the electric dipole moment (Table 3.1). A molecule with at least one non-zero electric dipole moment component will give rise to a rotational spectrum. When the dipole moment is zero by symmetry reasons there will be no observable transitions.

Table 3.1. Selection rules for the molecular rotation of an asymmetric rotor		
Dipole component	Allowed transition	Variation of the pseudo-quantum numbers
a	$ee \leftrightarrow eo$	$\Delta K_{-1} = 0, \pm 2, \pm 4 \dots$
	$oo \leftrightarrow oe$	$\Delta K_{+1} = \pm 1, \pm 3, \pm 5 \dots$
b	$ee \leftrightarrow oo$	$\Delta K_{-1} = \pm 1, \pm 3, \pm 5 \dots$
	$eo \leftrightarrow oe$	$\Delta K_{+1} = \pm 1, \pm 3, \pm 5 \dots$
c	$ee \leftrightarrow oe$	$\Delta K_{-1} = \pm 1, \pm 3, \pm 5 \dots$
	$oo \leftrightarrow eo$	$\Delta K_{+1} = 0, \pm 2, \pm 4 \dots$

We indicate some examples of rotational transitions in Table 3.2, classified according to the branch (*P*, *R* or *Q*) in which the spectroscopic transition is taking place.



Table 3.2. Asymmetric rotor transitions for low J values.

P or R brand	Type of transition	Q brand
$0_{00} \leftrightarrow 1_{01}$	a	$1_{11} \leftrightarrow 1_{10}$
$1_{01} \leftrightarrow 2_{02}$		$2_{02} \leftrightarrow 2_{21}$
$1_{11} \leftrightarrow 2_{12}$		$2_{12} \leftrightarrow 2_{11}$
$1_{10} \leftrightarrow 2_{11}$		$2_{21} \leftrightarrow 2_{20}$
$0_{00} \leftrightarrow 1_{11}$	b	$1_{01} \leftrightarrow 1_{10}$
$1_{01} \leftrightarrow 2_{12}$		$2_{02} \leftrightarrow 2_{11}$
$1_{11} \leftrightarrow 2_{02}$		$2_{12} \leftrightarrow 2_{21}$
$1_{10} \leftrightarrow 2_{21}$		$2_{11} \leftrightarrow 2_{20}$
$0_{00} \leftrightarrow 1_{10}$	c	$1_{01} \leftrightarrow 1_{11}$
$1_{01} \leftrightarrow 2_{11}$		$2_{02} \leftrightarrow 2_{12}$
$1_{11} \leftrightarrow 2_{21}$		$2_{12} \leftrightarrow 2_{20}$
$1_{10} \leftrightarrow 2_{02}$		$2_{11} \leftrightarrow 2_{21}$

3.1.3 Centrifugal distortion

Actual molecules are not rigid, so several bonding effects due to rotation have to be taken into account to reproduce the experimental spectra. In particular, the centrifugal forces associated to molecular rotation may produce a slight stretching in the chemical bonds and certain deformation in the molecular angles. The result is an increment in the moments of inertia which leads to a decrease in the rotational constants, so a reduction in the energy gap between the rotational levels is also induced. The theory of the centrifugal distortion has been studied by Watson [24]. The centrifugal distortion terms in the Watson Hamiltonian (asymmetric reduction) can be expressed to fourth order as

$$H_{cd}^{(A)} = -\Delta_J J^4 - \Delta_{JK} J^2 J_z^2 - \Delta_K J_z^4 - 2\delta_J J^2 (J_x^2 - J_y^2) - \delta_K [J_z^2 (J_x^2 - J_y^2) + (J_x^2 - J_y^2) J_z^2]$$

where we introduce five quartic centrifugal distortion constants labeled as Δ_J , Δ_{JK} , Δ_K , δ_J and δ_K . In case of larger contributions to centrifugal distortion (usually observable at high quantum numbers) higher-order terms can be introduced.



3.1.4 Nuclear quadrupole coupling

Several hyperfine interactions can be detected in rotational spectra by a splitting of the rotational transitions into several components. In our work we have observed nuclear quadrupole coupling interactions. This kind of hyperfine effect is an electric effect originated by the interaction between the quadrupolar moment (Q) of a particular nucleus (here chlorine) and the electric field gradient at the position of the quadrupolar nucleus generated by the rest of the charges of the molecule [18-20]. This interaction is observable when nuclei present a nuclear spin angular momentum larger than $\frac{1}{2}$, which is common in many organic molecules with nitrogen (^{14}N : $I=1$), chlorine (^{35}Cl : $I=3/2$) or other atoms. The quadrupolar moment can be visualized as a non-spherical charge distribution around the nucleus. This interaction produces a coupling of angular momenta, so the nuclear spin (I) adds to the rotational angular momentum (J), generating a total angular momentum of $F=I+J$, with a new associated quantum number $F=I+J, I+J-1, \dots, |I-J|$.

The nuclear quadrupole coupling introduces a new selection rule in F . If we combine the selection rules for the rigid rotor, $\Delta J=0, \pm 1$, with the condition that the nuclear spin does not change in the transition, $\Delta I=0$, the selection rules for the quantum number F must be:

$$\Delta F=0, \pm 1$$

The nuclear quadrupole coupling interaction generates a splitting in the energy levels, producing a hyperfine structure in the rotational spectrum, in which each transition may be split into several components. In some cases these transitions are so close that high resolution techniques are required. In other cases the splitting can be very large (even GHz).

The determinable properties associated to the nuclear quadrupole coupling are the coupling constants χ_{ij} :

$$\chi_{ij} = eQq_{ij}$$



where Q is the quadrupolar moment and q is the electric field gradient

$$q_{i,j} = \frac{\partial^2 V}{\partial i \partial j} \quad i, j = a, b, c$$

These coupling constants are components of the nuclear quadrupole coupling tensor:

$$\chi = \begin{pmatrix} \chi_{aa} & \chi_{ab} & \chi_{ac} \\ \chi_{ba} & \chi_{bb} & \chi_{bc} \\ \chi_{ca} & \chi_{cb} & \chi_{cc} \end{pmatrix}$$

The comparison between the experimental nuclear quadrupole constants and those predicted by theoretical methods constitute a unique tool for conformational identification, allowing us to assign without confusion structures with very similar rotational constants.



3.2 Computational Methods

There is a wide range of theoretical and computational methods, with very different strengths and computational costs [21]. The selection of the most appropriate theoretical methods is a difficult problem which depends to a large extent on the molecular size.

Widely speaking three different categories are possible:

1. Molecular Mechanics (MM)
2. Semi-empirical quantum mechanics
3. Ab initio and density-functional quantum mechanics

These methods are discussed below separately. In the course of our work we used both MM and ab initio and DFT methods. The computational results will be presented in chapter 4.

3.2.1 Molecular Mechanics

Molecular Mechanics (MM) is an empirical method appropriate for molecular systems of very large size, like proteins or macromolecules, where the number of atoms is very large (for example 100.000 atoms).

Molecular mechanics uses the equations of classical mechanics in combination with empirical potential functions accounting for intramolecular covalent and non-covalent interactions, like bonding, bending, torsion, etc. Many relevant terms, like electronic energies or quantum effects, are not considered. For this reason this kind of methods are very fast but generally inaccurate. This methodology is thus a first approximation to molecular structural parameters, and is available in many computer programs like *Hyperchem* [25] or *Macromodel* [26].

The selection of an adequate force field is the most important point in MM, as different methods produce very distinct results. Experimental force fields used in MM are



designed to reproduce either a particular set of atomic types or specific molecular parameters. Some of the typical force fields are:

- MM+ (Molecular Mechanics, Allinger 1977). MM+ is a refined proprietary version of original Allinger's MM2 and is implemented in HyperChem. MM2 was originally the force field with the most diverse parameter set (mostly from X-Ray structures). It is appropriate for organic molecules with no transition chemical elements.

- AMBER (Assisted Model Building and Energy Refinement, Weiner 1984): it uses the *united atoms* approximation. This approximation does not consider explicitly non-polar hydrogen atoms, it just increases the radius of the atom joined to it, treating it as a whole. It is appropriate for large organic molecules, like proteins.

- BIO+CHARM (Chemistry at Harvard Macromolecular Mechanics, Karplus 1983): it is based in the same principles as AMBER. It was designed for biomolecules and biopolymers.

- OPLS (Optimized Potentials for Liquid Simulations, Jorgensen 1988): It includes the united atoms approximation. It was developed for the study of proteins and biomolecules in condensed phases.

- MMFFs (Merck Molecular Force Field): it was designed for small organic molecules. It includes cross terms with no-truncation, getting a better representation of the molecular systems.

In this work we used only MMFF [27], mostly because of previous experience of the group has proved to be a dependable method for organic molecules, generating a good description of the PES. We ran our calculations using Macromodel, which implements MMFF and other MM methods (AMBER, BIO+CHARM, etc).

The great advantage of MM methods is their low computational cost, so performing a conformational search is very fast. Since the objective of the conformational search is to carry out a survey of the PES reasonably detailed, these methods may be combined with one or several search algorithms to generate a large number of starting structures. The low accuracy of the MM results is not a serious problem in this context, as all the structures



generated in the conformational search are later reoptimized using high-level ab initio or DFT methods.

3.2.2 Conformational search

The objectives of the conformational search are the systematic exploration of the PES, identifying all possible minima representing the stationary structures. There are several methods for conducting a conformational search and all of them need to be complemented with molecular modelling techniques. In our case, we combine the conformational search with MM methods for reasons of speed.

We used two conformational search algorithms implemented in Macromodel:

1. Monte-Carlo Multiple Minimization (MCMM) procedures
2. Large-Scale Low-Mode (LLMOD)

Both methods can be classified as procedures that accumulate changes, in the sense that a collection of conformations is built during the search in which conformations generated initially are used for subsequent search steps [26].

The Monte-Carlo MCMM method is a random or stochastic method. Each MCMM step consists of: a) selection of an existing conformer; b) introduction of random changes (including dihedral angles for rotatable bonds and translation of molecules in clusters); c) sampling of possible rings (breaking of ring bonds, followed by rotation of single bonds and reformation of the bond), and d) postprocessing of the structures. In the final step all the probed conformations are minimized within an energy window checking for redundancy and stereochemistry. The MCMM is a very general method that can be applied to small and large structures. It is also generally very effective. However, searches can be long and CPU intensive.

The large-scale low-mode LLMOD method uses low frequency modes to construct conformational changes. This method can be applied independently or in combination with MCMM. In the LLMOD method the algorithm: a) selects an existing conformer; b) generates



normal modes; c) select a normal mode and amplify the mode to generate a very different structure and d) postprocessing of the structures. Postprocessing is similar in both cases. The strengths of the LLMOD method is that it can detect some conformations not obvious in the random searches, but it is not effective in sampling translations and rotations in molecular complexes.

3.2.3 Semiempirical methods

Semiempirical methods are those that solve approximately the Schrödinger equations, partially including some empirical parameters. We did not use semiempirical methods in this work.

3.2.4 Ab initio and Density-Functional Theory:

Ab initio and density-functional theory are rigorous molecular orbital methods that solve exactly the quantum mechanical calculations associated to the time-independent non-relativistic electronic Hamiltonian in the Born-Oppenheimer approximation [28]. It is important to note that the accuracy of these methods depends on the quality of the approximations assumed to describe the atomic orbitals and the electronic correlation.

There is a large hierarchy of ab initio methods, with very different computational costs (figure 3.2) [21]. Usually it is convenient to use the largest model compatible with reasonable computational times. The simplest approach is the Hartree-Fock (HF) approximation, in which the instantaneous coulombic electron-electron repulsion is not considered explicitly and is replaced by an averaged value. This calculation method uses the variational principle and tends to a limit value called HF limit as the size of the basis set is increased. The HF method is nowadays obsolete, but it is used as a first step for more advanced calculations. The methods including electron correlation are called post-HF.

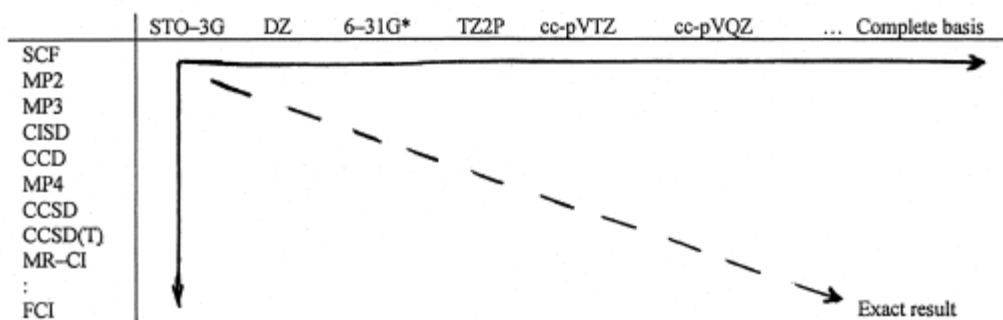


Figure 3.2 Different ab initio methods and basis sets and their accuracy in the calculations. The horizontal axis represents the basis set used to describe the atomic orbitals. The vertical axis represents the different treatment of the electron correlation.

One of the most common post-HF calculations is the Møller-Plesset method [29]. This method uses the Rayleigh–Schrödinger perturbation theory (RS-PT), usually to second (MP2), third (MP3) or fourth (MP4) order (the correlation potential does not contribute to the first-order electronic energy). Nowadays the MP2-MP4 methods are relatively standard for the calculations of small systems and are implemented in many software packages (in our case all ab initio calculations used Gaussian09 [30]). The MP methods are not always convergent at high orders, so very often only the MP2 method is used to reduce the computational costs. Most of the calculations in our work were MP2.

In some cases the accuracy of the MP methods may not be sufficient. In these cases other post-HF methods can be convenient. In our case we conducted some calculations using coupled-cluster (CC) theory. CC theory includes several numerical methods that construct multi-electron wavefunctions using the exponential cluster operator to account for electron correlation [31]. Some of the most accurate calculations for small to medium sized molecules use this method. The cluster operator can be written to different approximations. The simplest methods used single and double excitations (CCSD). For a better accuracy triple excitations can be added. In the relatively common CCSD(T) method the coupled cluster theory is used with a full treatment for singles and doubles excitations, while an estimate to



the connected triples contribution is calculated non-iteratively using Many-Body Perturbation Theory. Some CCSD(T) calculations have been done during our work.

Alternatively to *ab initio* methods, there has been a large development of density-functional methods or DFT [32]. In DFT theory the properties of a many-electron system can be determined by using functionals, (functions of another function), which in this case is the spatially dependent electron density. The name density functional theory comes from the use of functionals of the electron density. DFT has been very popular since the 1970s. However, DFT was not considered accurate enough for calculations in quantum chemistry until the 1990s, when the approximations used in the theory were greatly refined to better model the exchange and correlation interactions. The most important point of DFT theory is that the computational costs are relatively low when compared to traditional methods, such as HF and other methods based on the complex many-electron wavefunctions.

A critical point in using DFT methods is the selection of an appropriate functional. Different functionals account for electron correlation and other interactions in slightly different ways, so their performance may be very different. One of the most common DFT methods is B3LYP (Becke, three-parameter- Lee-Yang-Parr) [33]. The B3LYP method is a hybrid functional, i.e., they incorporate a portion of exact exchange energy from HF theory and another exchange and correlation terms from empirical or theoretical sources. In B3LYP the functional is defined in terms of three parameters obtained from fittings of the B3PW91 functional results to a set of atomization energies, ionization potentials, proton affinities and total atomic energies. The resulting functional is very fast but it has some deficiencies. In particular, it does not account for dispersion interactions, so it cannot be used in studies of intermolecular complexes.

An alternative to the B3LYP functional introduced since 2005, are the Minnesota functionals developed by Truhlar, generally denoted M04, M05, M06, etc [34]. These functionals are called meta-GGA, because they include terms that depend on the kinetic energy density and are based on flexible functionals parametrized from benchmark



databases. The MOx functionals are intended to have a general applicability in Chemistry and, in particular, they empirically account for dispersion interactions. This property makes these functionals very useful for the study of stable molecules or intermolecular complexes where dispersion plays a significant role. These functionals have also a very reduced computational cost, so they are very effective for practical purposes. Several of these functionals are incorporated in different software packages. In particular we have used the M06-2X functional as implemented in Gaussian09 [30].

All the available computational methods described above must be combined with an adequate set of basis functions. A set of basis functions is a representation of the atomic orbitals needed to create the molecular orbitals. Because of computational costs the atomic orbitals must be represented by a finite set of basis functions. When a finite basis set is expanded towards an infinite set of functions the basis set is said to approach the basis set limit, which represents the maximum possible accuracy. The basis sets are commonly expressed as a finite number of atomic orbitals, centered at each nucleus. Initially atomic orbitals were described with Slater orbitals, but it was proved by Pople that it is possible to obtain a large reduction in computer time using Gaussian basis functions.

There are many possible basis sets. Since we used the computational methods as an auxiliary method to perform the spectral analysis we did not try different basis sets, but relied on previous studies applied to spectroscopic problems. Following previous experience we used in our calculations three Pople basis set denoted 6-31G(d,p), 6-311++G(d,p) and 6-311++G(2df,p), but results are indicated only for the last basis set [35]. These basis sets are called split-valence, meaning that there are multiple basis functions corresponding to each valence atomic orbital. The first one describes each internal orbital with six Gaussian functions and each valence orbital is double-zeta (two functions), one of them is a contraction of three Gaussian functions and the other one is a primitive Gaussian function. The second one has a better description of the valence orbitals with three contractions of Gaussian functions (triple zeta). The three basis sets include polarization functions for both heavy and light atoms like hydrogen, together with diffuse functions in the second and third case.



4. Results

4.1 Computational modelling

The study of conformational problems arising from hindered internal motions is a classic topic in structural Chemistry [36]. Even for small molecules the internal rotation around single bonds may result in a large number of isomers (or rotamers), and a detailed description of the conformational distribution requires investigating both the spectral properties and the potential energy surface (PES) of the molecule.

Among the experimental methods the investigation of the pure rotational spectrum in the microwave region provides the most accurate description of the molecular structure in the gas phase [4], since the sensitivity of the moments of inertia to the mass distribution results in independent spectra for all species in the sample.

However, the experimental investigation requires a previous understanding of the PES, which can be complicated when the molecules present too many conformers. In these cases chemical intuition does not allow us to predict systematically all the stable conformations, so theoretical calculations are necessary to determine the preferred structures and their molecular properties.

In this work we have carried out a theoretical and experimental investigation of the volatile anesthetic enflurane. As mentioned in chapter 1 this work follows previous studies on the related molecules sevoflurane [7], isoflurane [8] and desflurane [9]. Comparisons will also be made with previous studies on enflurane, in particular the gas-electron diffraction study of Oberhammer [10]. In this chapter we present the computational results. The analysis of the rotational spectrum appears in section 4.2.

The theoretical calculations proceeded in two steps:

a) Conformational search

These calculations are described in 3.1 and used Molecular Mechanics to obtain a systematic description of the most stable conformations.



b) Ab initio and Density-functional Theory (DFT) calculations

These methods are described in 3.2 and are used to obtain accurate molecular properties and spectral predictions.

4.1.1 Conformational search

The possible conformations of the molecule were generated initially through an extensive conformational search using Molecular Mechanics (MM). MM uses classical mechanics combined with a particular force field representing the covalent and non-covalent intramolecular interactions like bonding, bending, torsion, etc. There are many force fields, some of them specific for particular types of molecules. In this work we used the Merck Molecular force field (MMFF) [27], which is implemented in the program MacroModel [26].

MM needs to be complemented with algorithms for conformational search. In this work we used a combination of two methods, the Large-scale Low-Mode (which uses low frequency modes to construct conformational changes) and the Monte-Carlo Multiple Minimization procedures, which are also implemented in MacroModel. These methods have been very effective in the past for similar molecules done in our group.

The conformational search followed an iterative approach that began with a series of surveys of the many possible molecular structures. The process is repeated until no additional new structures are obtained. We imposed no geometry constraints so all molecular parameters were allowed to vary. The search algorithm automatically checks for redundancies and mirror structures. These surveys generated hundreds of structures. The most relevant structures were later selected on the basis of their calculated relative energies. The lowest energy conformers used initially a cut-off 25 kJ mol^{-1} , and produced a total of 43 different conformations.



The conformational energies and structures obtained by MM are not expected to be accurate. However, this kind of calculation puts special attention to conduct a comprehensive survey of the PES.

All the structures obtained by MM were later reoptimized by ab initio and density-functional theory.

4.1.2 Density-Functional-Theory and ab initio calculations

In order to obtain accurate results for the spectroscopic investigation all the structures obtained with MM were reanalyzed with ab initio and DFT molecular orbital calculations. These calculations involve two steps:

a) Structural optimization

All structures are fully reoptimized with no geometrical constrains. The resulting conformational energies produce the final conformational distribution.

b) Vibrational frequency calculations

Vibrational frequency calculations have two objectives: establishing the character of the stationary points of the PES (either local minima or transition states) and determining the zero-point energy corrections and the thermochemical parameters, in particular the Gibbs free energies.

One of the most important points in molecular orbital calculations is the adequate selection of the calculation method and the atomic orbitals basis sets. Previous studies on enflurane by Oberhammer [10] have used the Hartree-Fock approximation (HF/3-21G(d)), the B3PW91 density functional and second-order Moller-Plesset (MP2) perturbation theory (both with the 6-311G(2d) basis set).

In our case we decided to use first the M06-2X DFT method and MP2. The M06-2X functional has been introduced recently [34], and its main advantage is that it empirically accounts for dispersive interaction. Previous experience in our group has shown that it is very effective in terms of computational cost and at the same time it provides accurate

results for organic molecules. On the other hand, MP2 [29] is a pure ab initio method which is expected to give a good balance between spectroscopic accuracy and computational cost. At the end of this work a few more calculations used a more sophisticated coupled-cluster method (CCSD(T)) [31] to try to resolve the small energy differences between the most stable conformations, as described below.

The atomic basis set chosen in this work was the Pople 6-311++G(2df,p). This triple- ζ basis set contains polarization and diffuse functions and was selected because it has been used in previous works of the related molecules sevoflurane [7] and isoflurane [8], making comparisons more meaningful. Some calculations used the Dunning's aug-cc-pVTZ basis set for comparison. All ab initio and DFT calculations used the Gaussian 09 [30] suite of programs.

We present in Table 4.1 the results of the conformational search (conformers are labelled sequentially as 1, 2, etc.). For each conformer we tabulated the electronic energy, three most relevant dihedral angles and the rotational constants. For simplicity we indicate only the MP2 energies. Atomic labelling for the molecule is shown in Figure 4.1 (S-stereoisomer). We additionally compared in this table our results with the previous theoretical search conducted by Oberhammer [10] (labelled with roman numerals, I, II, III, etc). For additional clarity we present graphically the results of the MP2 conformational distribution in Figure 4.2.

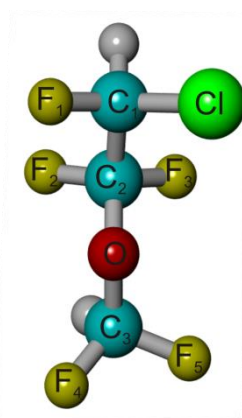


Figure 4.1. Atomic labelling of the (S-) enflurane molecule.



There are several important conclusions from the conformational search. The 43 different conformations obtained from MM converged to only 26 different conformers with energies lower than 25 kJ mol^{-1} . There are six most stable conformations (1, 2, ..6), which are very close in energy ($< 1 \text{ kJ mol}^{-1}$). A second group of conformations (7-21) appears at relative energies of $5\text{-}10 \text{ kJ mol}^{-1}$. Finally a third group of structures (22-27) are located at relative energies larger than 15 kJ mol^{-1} .

The six most stable conformations of enflurane share a heavy-atom (C-O-C-C) near-planar skeleton, with the terminal chloro-fluoro-methyl group (CHClF) adopting three alternative staggered conformations, as shown in Figure 4.3.

The nomenclature used in this work is based in the definition of the torsion angles.¹ We defined the molecular conformations with the same torsion dihedrals used in the previous work by Oberhammer [10]: $\phi_1(\text{Cl-C}_1\text{-C}_2\text{-O})$, $\phi_2(\text{C}_1\text{-C}_2\text{-O-C}_3)$, $\phi_1(\text{C}_2\text{-O-C}_3\text{-H})$. Those dihedrals are tabulated in Table 4.1 for all stable conformations.

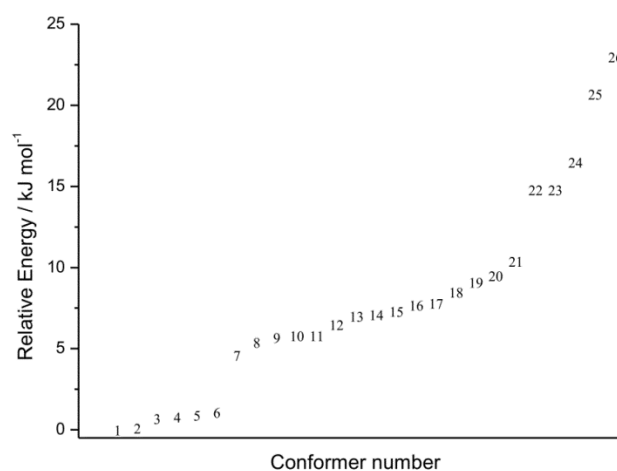


Figure 4.2. Conformational distribution of enflurane according to Table 4.1.

¹ The torsion angle of the atom chain A-B-C-D is the dihedral between the planes containing the A-B-C and B-C-D atoms. In a Newman projection, the torsion angle (with absolute value between 0° and 180°) is defined between two specific groups, one closer and one remote to the observer. The torsion between A and D groups is positive if the clockwise rotation of the A-B bond ($<180^\circ$) will eclipse the C-D bond. It is considered negative if the rotation required to get that situation is anti-clockwise. In macromolecular chemistry T, C, G+, G-, A+ and A- symbols are recommended for antiperiplanar, synperiplanar, \pm synclinal and \pm anticlinal orientations, respectively.

**Table 4.1.** Conformational search of enflurane using ab initio methods (MP2/6-311++G(2df,p)).

Conf	Ref. 10	$\Delta E / \text{kJ mol}^{-1}$	$\phi_1(\text{Cl-C}_1\text{-C}_2\text{-O})$	$\phi_2(\text{C}_1\text{-C}_2\text{-O-C}_3)$	$\phi_3(\text{C}_2\text{-O-C}_3\text{-H})$	A / MHz	B / MHz	C / MHz
1	II	0.0	-62.3	-174.4	-20.5	1865.2	727.4	609.4
2		0.1	-63.8	+176.4	+19.2	1825.5	730.9	629.3
3	III	0.7	+60.7	-176.8	-22.3	1643.6	749.9	694.5
4	IV	0.8	+59.4	+174.0	+20.5	1691.7	743.4	677.8
5	I	0.9	-178.9	+176.2	+22.0	2389.6	636.1	578.4
6		1.1	-177.8	-174.8	-19.0	2401.6	626.5	591.9
7	VIII	4.6	+55.6	+68.9	+18.7	1467.5	925.2	760.3
8	VI	5.4	-176.3	-75.6	-10.9	2116.9	728.2	621.2
9		5.7	-179.1	-90.7	+22.1	2160.3	701.7	616.6
10		5.8	+62.2	-159.7	-163.6	1770.0	845.3	704.7
11		5.8	+58.7	+158.2	+163.4	1942.3	755.8	707.2
12	XI	6.5	-65.0	+159.3	+164.2	1854.5	843.9	668.9
13		7.0	-60.4	-158.5	-162.1	2050.3	723.0	669.1
14	X	7.1	+177.4	+159.0	+163.9	2321.7	721.8	637.4
15	XIII	7.3	-56.9	-82.1	-53.6	1606.0	829.2	709.1
16		7.7	+62.0	-112.6	+39.1	1508.9	861.3	719.5
17		7.8	-179.4	-160.0	-162.0	2333.8	674.7	651.6
18	XIV	8.5	+175.9	+85.3	+54.2	2053.2	700.0	661.3
19	XV	9.1	-54.6	-85.4	+166.1	1771.4	827.9	729.9
20		9.5	+50.7	+51.4	-55.0	1416.1	906.2	800.3
21		10.4	-178.1	+50.7	+165.3	1722.5	854.9	775.1
22		14.8	+172.4	+37.6	-67.9	1998.4	718.3	686.7
23		14.8	+53.9	+57.7	+164.5	1430.0	1082.3	858.9
24		16.5	-166.9	-51.5	-167.3	1862.2	857.8	744.6
25		20.7	+79.6	-60.4	-161.9	1258.5	1164.8	931.7
26		23.0	+56.7	-84.0	+168.3	1448.4	1074.3	812.3

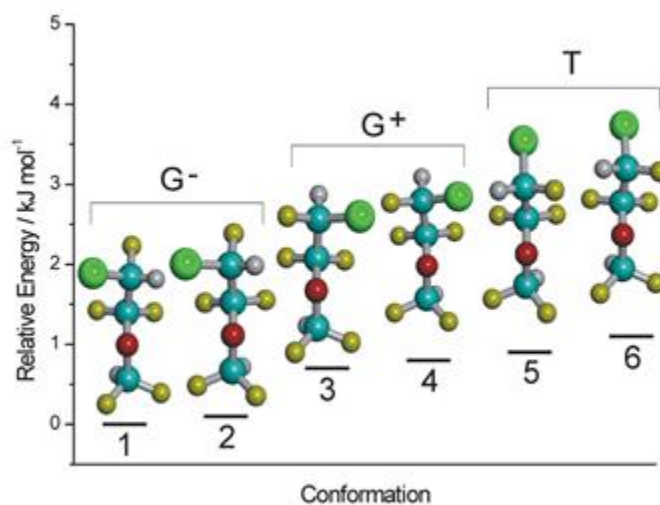


Figure 4.3. The six lowest-lying conformers of enflurane (MP2/6311++G(2df,p) electronic energies)

Using the previous dihedrals the six most stable conformations of enflurane differ mostly in the *trans* (T: $\phi_1(\text{Cl-C}_1\text{-C}_2\text{-O}) \approx 180^\circ$) or *gauche* orientation of the chlorine atom, either G^- ($\phi_1(\text{Cl-C}_1\text{-C}_2\text{-O}) \approx -60^\circ$) or G^+ ($\phi_1(\text{Cl-C}_1\text{-C}_2\text{-O}) \approx +60^\circ$). The second dihedral is always *trans* ($\phi_2(\text{C}_1\text{-C}_2\text{-O-C}_3) \approx 180^\circ$). Finally, the terminal hydrogen in the difluoromethyl group is not completely *cis* to the carbon chain, but prefers dihedrals of ca. $\phi_3(\text{C}_2\text{-O-C}_3\text{-H}) \approx \pm 20$ degrees. The combination of three staggered orientations for the chlorine atom and two orientations for the terminal difluoromethyl hydrogen produces the six most stable conformations of the molecule. In other words, the preferred conformations of the molecule maintain a near planar carbon skeleton and the internal rotation of the chlorofluoromethyl group generates three alternative orientations for the chlorine atom. The six preferred conformations of enflurane are shown in detail in Figure 4.4.

A consistent notation for the enflurane conformers should include all three (ϕ_1, ϕ_2, ϕ_3) dihedrals, for example G^-TG^- for the global minimum in Table 4.1 and Figure 4.3. However, since we will be mostly concerned with the six low-lying conformations we will indicate in most cases only the chlorine atom dihedral (ϕ_1). According to the



MP2 results one of the *gauche* conformers (G^-) is the global minimum of the molecule, while the second *gauche* form (G^+) and the *trans* (T) species are slightly higher in energy (ca. 0.7-1 kJ mol⁻¹). However, the energy difference between the G^+ and T conformations and between both structures and the global minimum G^- is so small that it could be possible that they are not calculated accurately at our level of calculation. We have thus conducted more calculations with different methods, as described below.

A second problem arises because of the presence of two possibilities for the difluoromethyl hydrogen for each orientation of the chlorine atom, like the pair G^-TG^- and G^-TG^+ . These two possibilities are practically isoenergetic in our predictions, so it is very difficult a priori to establish which one could be more stable. However, we can reasonably expect that the potential energy barrier between the two hydrogen positions will be low. In these conditions, previous experiments in molecular jets have proved that the supersonic expansion produces a conformational relaxation to the most stable species and the higher energy form remains unpopulated [37]. For this reason we would expect to observe only one of the two possibilities for the hydrogen atom.

In consequence, the experimental data will be finally determinant to establish the validity of the theoretical predictions.

Another indication of the difficulty to model the relative energies between the most stable conformations is the fact that our conformational energies differ from those of Oberhammer [10]. In that work the global minimum is conformation T using the B3PW91 method and G^- with MP2. Conformers 2, 6, 9, 10, 11 and others are also missing in that work. A comparison of both predictions is given in Table 4.1.

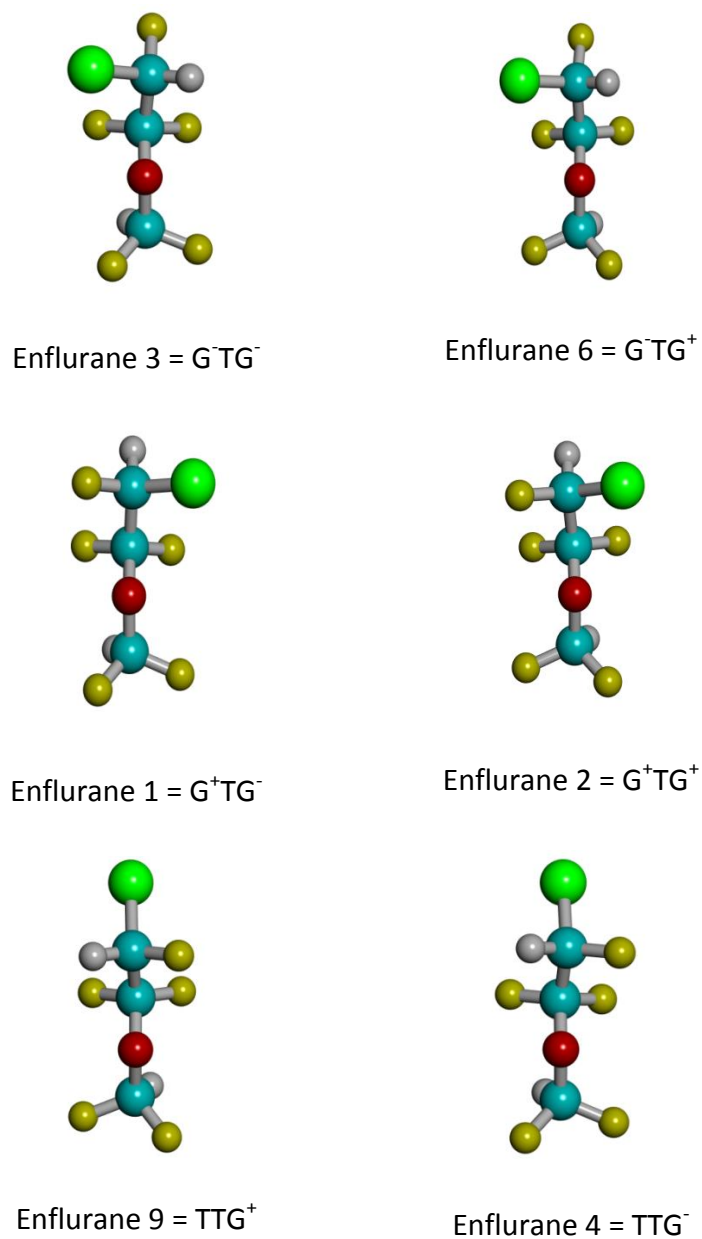


Figure 4.4. The six lowest-lying conformers of enflurane.

In order to improve the theoretical predictions for the conformational energies of the most stable conformers we ran additional calculations using the coupled-cluster method (singles, doubles and triples), denoted CCSD(T). This method is computationally more expensive, so we ran only single-point energy calculations at the



geometries of the MP2 method. We used the 6-311++G(d,p) basis set. The results of these calculations are shown in Table 4.2.

Finally, once the conformational landscape was understood, we tabulated the molecular properties relevant for the rotational study. We show in Table 4.2 the rotational constants, centrifugal distortion terms and nuclear quadrupole coupling parameters, which were instrumental for the analysis of the spectrum.

The data obtained from the MP2 and CCSD(T) calculations on electronic energies show that the tendency of the most stable conformers is the same, so both methods reveal the same information. However, it is worth mentioning that the relative free energy of the different conformers does not follow the same tendency. The detected species remain as the most stable conformations, but those conformers with different orientation of the difluoromethyl group, previously very close in energy, shows now a much higher value. The same happens for the three *gauche* and *trans* conformer pairs. Therefore, the entropic contributions to the free energy must be the reason of this variation. Previous experiments have shown the importance of using Gibbs free energies instead of electronic energies to correctly predict the conformational distribution [38].

**Table 4.2.** Ab Initio predictions for the most stable conformations of enflurane. (MP2/6-311++G(2df, p))

	Conformer G ⁻ <i>G⁻TG⁻</i>	Conformer G ⁻ <i>G⁻TG⁺</i>	Conformer G ⁺ <i>G⁺TG⁻</i>	Conformer G ⁺ <i>G⁺TG⁺</i>	Conformer T <i>TTG⁺</i>	Conformer T <i>TTG⁻</i>
<i>A</i> / MHz ^a	1865.67	1771.38	1643.63	1606.03	2389.65	2116.91
<i>B</i> / MHz	727.54	827.85	749.86	829.23	636.08	728.22
<i>C</i> / MHz	609.31	729.85	694.49	709.11	578.37	621.22
Δ_J / kHz	0.039	0.20	0.079	0.19	0.021	0.045
Δ_{JK} / kHz	-0.024	-0.89	-0.095	-0.027	0.071	-0.041
Δ_K / kHz	0.39	1.77	0.35	0.17	0.18	0.35
δ_J / kHz	0.0095	0.081	0.0085	0.073	0.0038	0.010
δ_K / kHz	0.19	0.84	0.47	0.093	0.35	0.117
χ_{aa} / MHz	21.98	1.94	28.56	25.93	-43.78	-61.38
χ_{bb} / MHz	-54.37	-7.92	-59.32	-32.93	16.58	32.71
χ_{cc} / MHz	32.39	5.97	30.76	7.01	27.20	28.67
$ \chi_{ab} $ / MHz	31.98	-35.94	-28.16	-22.35	36.03	11.41
$ \chi_{ac} $ / MHz	8.19	-30.28	6.67	-14.27	-28.88	-27.25
$ \chi_{bc} $ / MHz	-19.92	-37.056	15.80	-45.79	13.05	1.24
$ \mu_a $ / D	0.12	1.04	0.63	1.17	0.31	1.04
$ \mu_b $ / D	0.28	-2.27	1.03	0.45	0.89	0.733
$ \mu_c $ / D	0.21	-0.03	1.73	1.43	0.09	-0.06
$ \mu_{TOT} $ / D	0.37	2.50	2.11	1.91	0.94	1.27
ΔE / kJ mol ⁻¹	0.0	0.57	0.7	1.13	0.9	1.4
ΔG / kJ mol ⁻¹	0.0	11.8	0.7	8.04	0.9	6.9
$\Delta E^{CCSD(T)}$ / kJ mol ⁻¹	0.0	0.25	0.26	0.79	1.14	1.24

^aRotational constants (*A*, *B* and *C*), electric dipole moments (μ_α , $\alpha = a, b, c$) and diagonal elements of the nuclear quadrupole tensor of ¹⁴N ($\chi_{\alpha\beta}$, ($\alpha, \beta = a, b, c$)) for conformer 1 optimized with ab initio methods. The centrifugal distortion constants are also shown (Δ_J , Δ_{JK} , Δ_K , δ_J and δ_K). The relative energies have been corrected with the zero-point energy (ZPE).

4.2 Spectral analysis.

This section discusses the analysis of the rotational spectrum of enflurane.

4.2.1 Conformer A

The rotational spectrum of enflurane was started at the *National Institute of Standards and Technology* (NIST) by Richard Suenram *et al.* in 1999 [39], using a Balle-Flygare Fourier-transform microwave (FTMW) spectrometer [40]. This preliminary study identified a single conformer, denoted here enflurane A. This work was not published.

Later on, our group extended the measurements on the parent species and the ^{37}Cl isotopologue of conformer A, and determined the nuclear quadrupole coupling parameters originated by the chlorine nucleus in both isotopologues [41]. However, many transitions remained unidentified.

In order to fully understand the rotational spectrum of enflurane our group has recently collaborated with the Brooks Pate group at the University of Virginia, where the broadband spectrum of enflurane has been recorded in conditions of high sensitivity in the bands 2-8 GHz and 6-18 GHz. These new experimental spectra were obtained with a chirped-pulse (CP-FTMW) spectrometer [42], and are shown in Figures 4.5 and 4.6. The work presented here has included the reanalysis of conformer A and the detection of new conformers and isotopologues using this experimental dataset and previous spectral data available in our group. The results of the spectral analysis will be later compared with the computational results of section 4.1 to produce a global description of the molecular properties of enflurane.

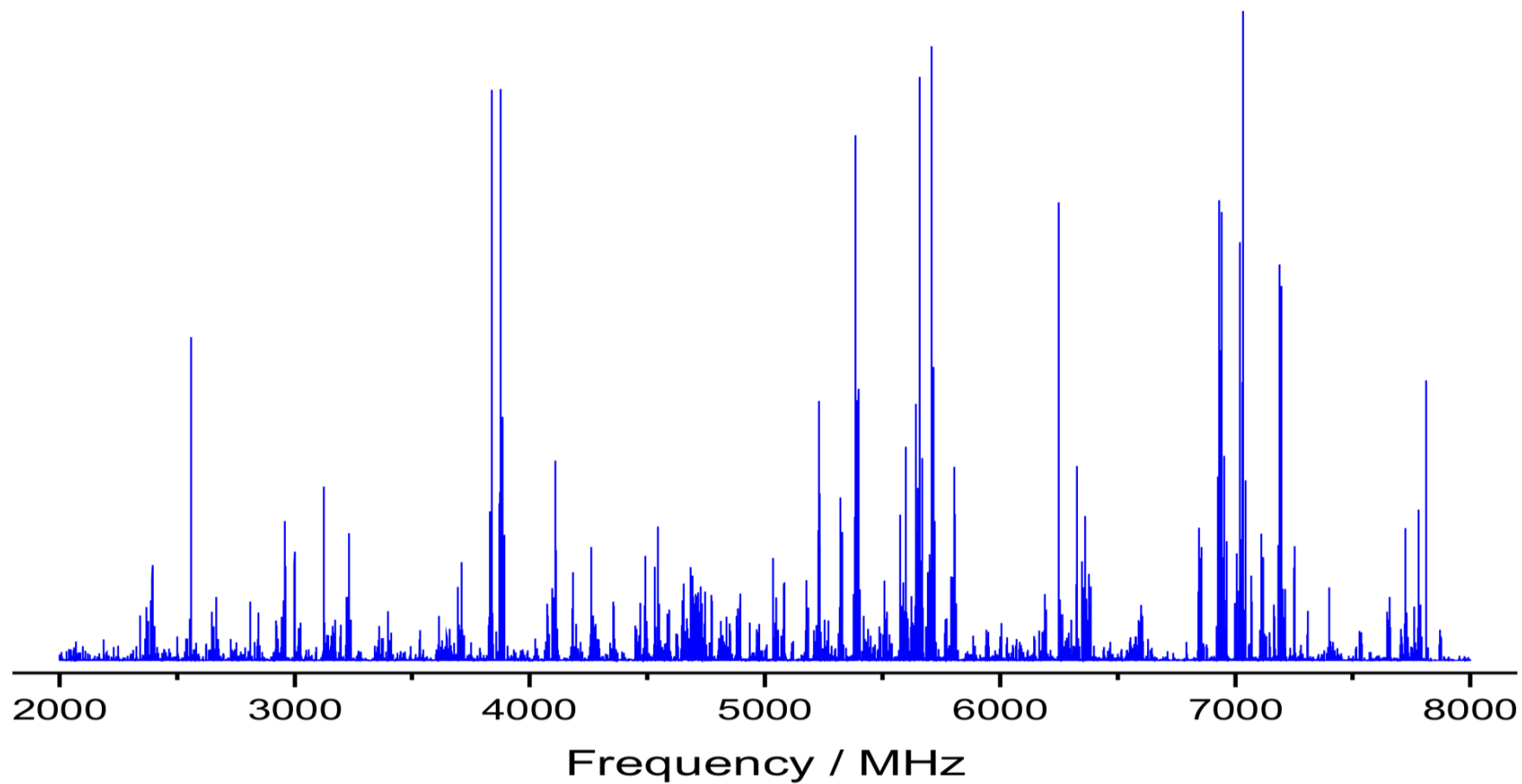


Figure 4.5. Experimental spectrum (2000-8000 MHz) obtained with a FTMW broadband spectrometer. Data recorded by the Pate group at the University of Virginia

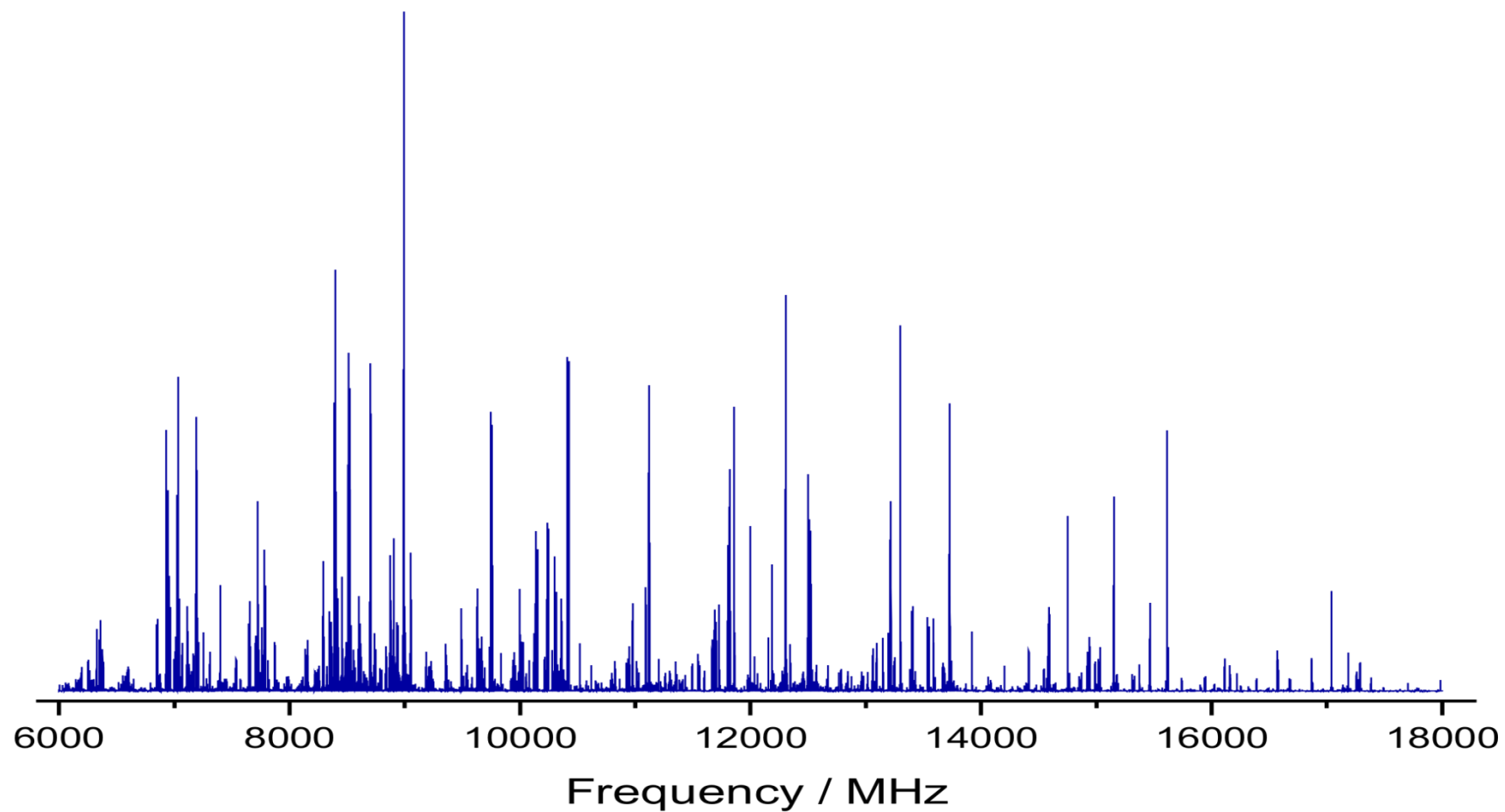


Figure 4.6. Experimental spectrum (6000-18000 MHz) obtained with a FTMW broadband spectrometer. Data recorded by the Pate group at the

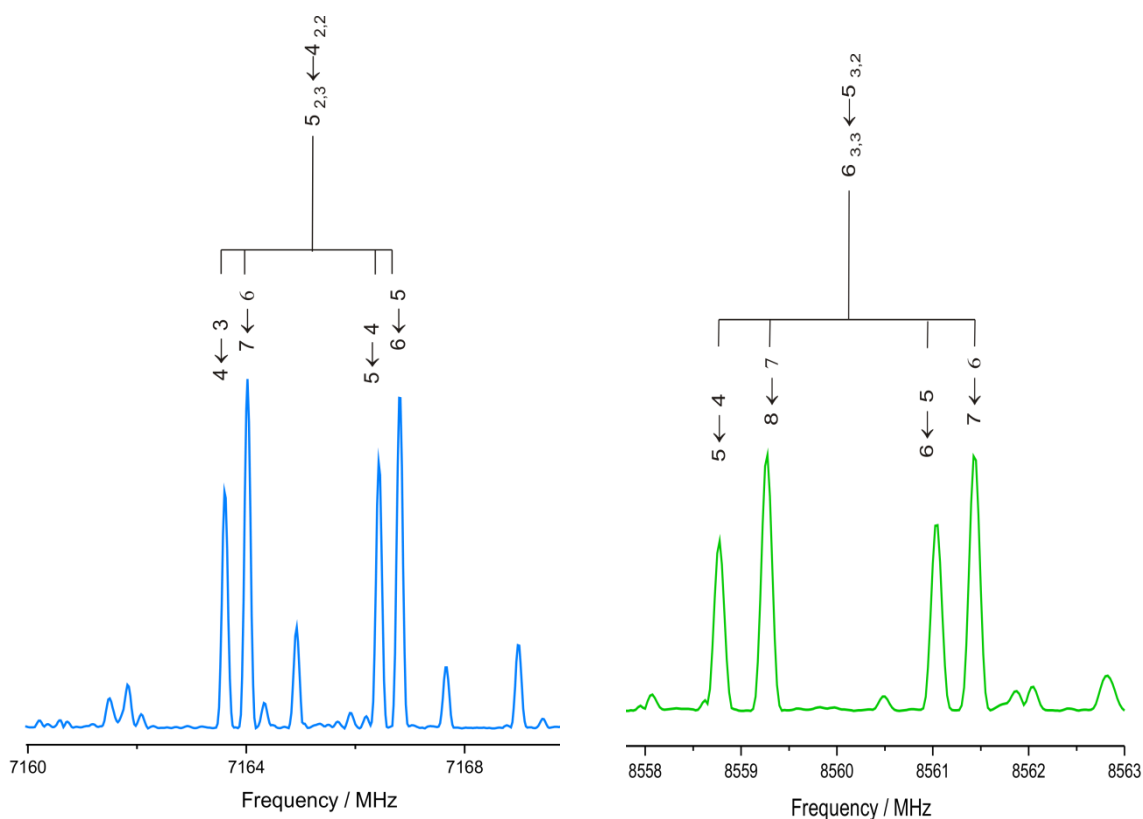
University of Virginia



The first task of the new analysis was a re-examination of conformer A. Since this conformer was previously assigned, the measurement of new transitions was straightforward. The procedure started from the previous rotational parameters and assigned lines, and continued with the measurements of an enlarged set of transitions. Finally, a total of 2119 transitions were fitted for the ^{35}Cl isotopologue of conformer A. The experimental transitions were weighted according to the experimental uncertainties (FTMW: 5 kHz; CP-FTMW: 150 kHz) and included all present and past data.

All lines in the spectrum exhibited nuclear quadrupole coupling hyperfine effects [18-20] due to the presence of the ^{35}Cl nucleus (nuclear spin $I=3/2$). The hyperfine effects are illustrated in Figures 4.7 and 4.8 for the $5_{3,3} \leftarrow 4_{2,2}$ and $6_{3,3} \leftarrow 5_{3,2}$ transitions, respectively. Typically each rotational transition is split into four more intense components, though several more weaker components are observable in some cases. The chlorine nuclear quadrupole effects usually spans several MHz. The corresponding determinable parameters are the elements of the nuclear quadrupole coupling tensor $\chi_{\alpha\beta}$, which are expressed with respect to the principal inertial axes ($\alpha, \beta = a, b, c$). The coupling tensor is related linearly to the electric field gradient at the quadrupolar nucleus, according to $\chi = eQq$.

Initially, only the diagonal elements of the coupling tensor ($\chi_{aa}, \chi_{bb}, \chi_{cc}$) were determined experimentally. However, this fit did not work very well as the number of transitions increased. For this reason we tried determining some of the out-of-diagonal coupling components ($\chi_{ab}, \chi_{ac}, \chi_{bc}$, since the tensor is symmetric). Finally, two out-of-diagonal coupling tensor elements (χ_{ab}, χ_{bc}) were determined (the sign of the non-diagonal elements is not determinable experimentally [18]).



Figures 4.7 and 4.8. Illustrations of nuclear quadrupole coupling hyperfine splitting in transitions of conformer A of enflurane.

The spectral analysis included all fourth-order (or quartic) centrifugal distortion constants (Δ_J , Δ_{JK} , Δ_K , δ_J , δ_K) [24]. Additionally, and because of the large number of measured transitions, we could determine additionally one sextic centrifugal distortion constant (L_J). In the final fit we used the Watson asymmetric (A) reduction Hamiltonian (I^r representation) [24]. The results of the fit for the ^{35}Cl species are shown in Table 4.3.

When the analysis of the ^{35}Cl species of enflurane A was done, we continued with the ^{37}Cl isotopologue of this conformer, which was analyzed similarly. These measurements are relatively easy because of the large natural abundance of this species (24.23 % [43]). Since we had also a previous assignment for this species the measurement of new transitions was again straightforward. Finally we fitted a total of 1341 transitions. The resulting rotational parameters are shown also in Table 4.3.

Table 4.3. Experimental results for conformer A of enflurane.

	³⁵ Cl-enflurane A	³⁷ Cl-enflurane A
<i>A</i> / MHz	1656.134474(93)	1640.53612(16)
<i>B</i> / MHz	740.909159(63)	730.734776(95)
<i>C</i> / MHz	683.074934(58)	671.970812(78)
Δ_J / kHz	0.38871(39)	0.40550(60)
Δ_{JK} / kHz	2.0630(13)	1.6930(27)
Δ_K / kHz	2.2850(21)	3.1987(64)
δ_J / kHz	-0.12885(11)	-0.12472(30)
δ_K / kHz	5.8002(78)	5.106(15)
<i>L_J</i> / mHz	-0.0621(41)	
χ_{aa} / MHz	27.6750(27)	21.0383(28)
χ_{bb} / MHz	-61.5755(37)	-47.9635(40)
χ_{cc} / MHz	33.9005(64)	26.9253(68)
$ \chi_{ab} $ / MHz	35.41(12)	-28.70(12)
$ \chi_{ac} $ / MHz	[0.0000]	[0.0000]
$ \chi_{bc} $ / MHz	-13.652(42)	-9.992(75)
<i>N</i>	2119	1341
σ / kHz	12.3	10.8

4.2.2 Conformer B

Once conformer A (³⁵Cl and ³⁷Cl) was removed from the spectrum, many transitions were visible, clearly indicating that other species were still present. Figure 3.5 shows a 2 GHz section of the initial spectral survey (blue trace) between 12 and 14 GHz, together with the remaining lines after subtracting the ³⁵Cl and ³⁷Cl enflurane A species (red and green traces, respectively). Some of the remaining transitions are considerably intense.

In order to assign new species in this spectrum we ran different simulations using the computational data of section 4.1, which predicted three lowest-energy species.



Additionally, we used the AABS graphical simulation program from Kisiel [44], which allows comparing the predicted and theoretical spectra. After inspection of the spectrum a particular cluster of transitions around 12450 MHz was noticeable. We present three spectral sections of these transitions in Figure 4.9. Using several trial predictions these transitions could be finally assigned to a set of μ_b -type Q -branch ($J \leftarrow J$) transitions of general formula $J_{4,K} \leftarrow J_{4,K+1}$ ($J=4-8$).

This species was denoted as enflurane B or conformer B. The analysis of the rotational spectrum was similar to conformer A and we present in Table 4.4 the rotational parameters for the ^{35}Cl and ^{37}Cl species, where we again accurately determined the rotational constants and all quartic centrifugal distortion parameters.

The spectrum of enflurane B was very sensitive to the non-diagonal terms of the nuclear quadrupole coupling tensor. Finally, all tensor elements were accurately determined.

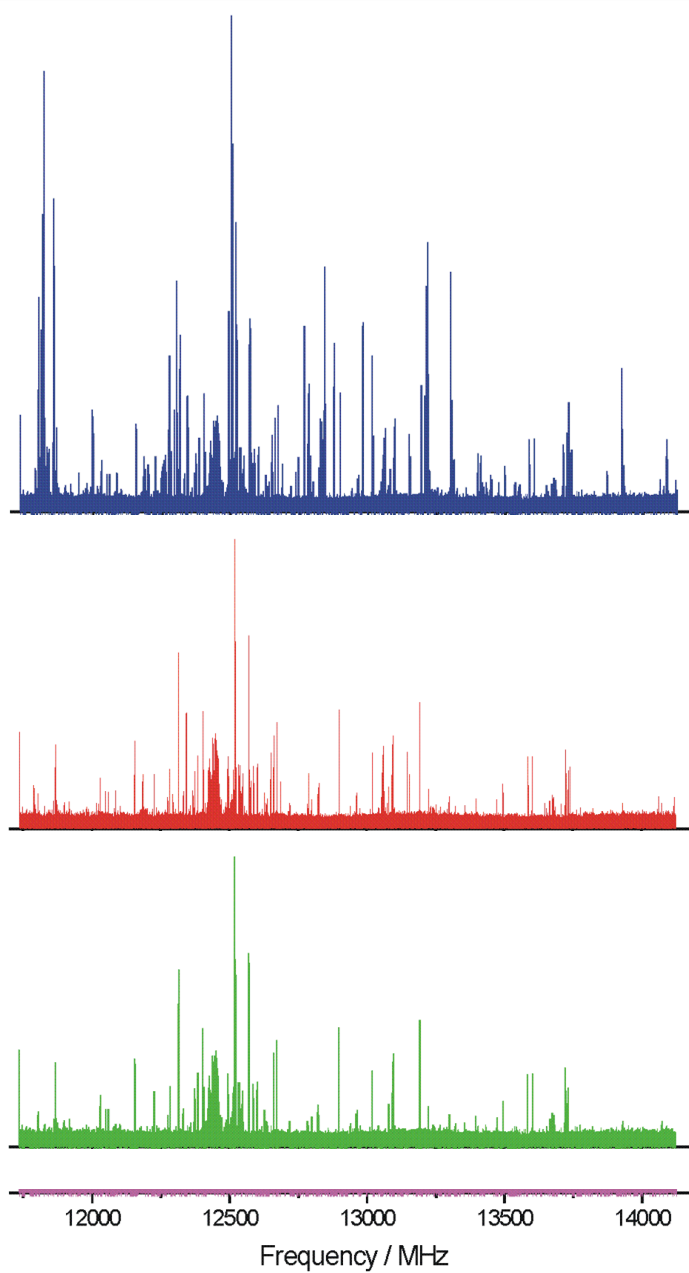


Figure 4.9. A section of the rotational spectrum of enflurane: full spectrum (blue trace), and resulting spectra after subtracting the transitions from the ^{35}Cl - and ^{37}Cl isotopologues of enflurane A (red and green traces, respectively). This spectral data were obtained from a survey scan using FTMW spectroscopy.

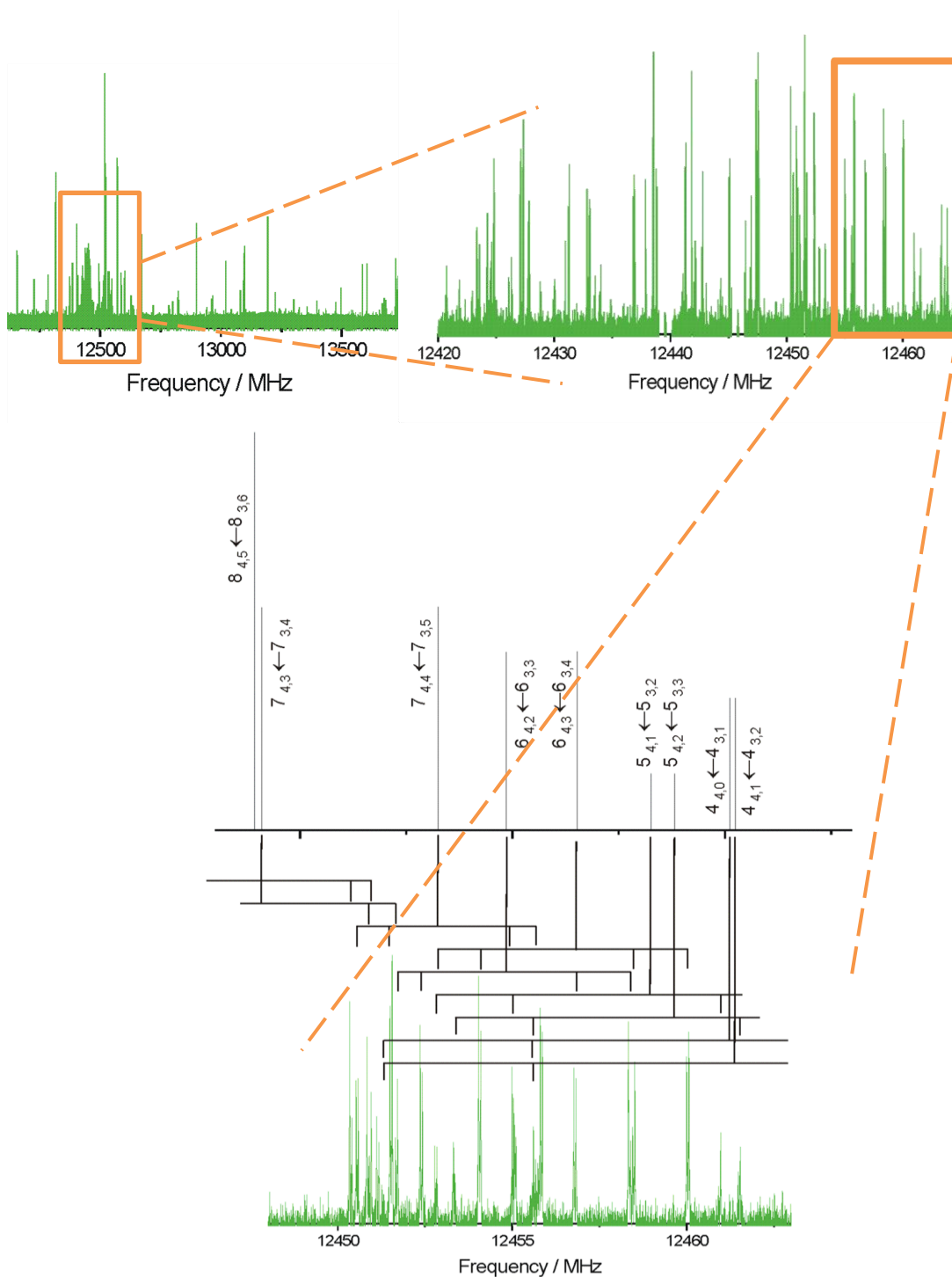


Figure 4.10. A group of bQ -branch transitions of enflurane which allowed the assignment of conformer B (transitions from conformer A had been subtracted). The experimental data correspond to the spectral section of previous figure.

**Table 4.4.** Experimental results for conformer B

	³⁵ Cl-enflurane B	³⁷ Cl-enflurane B
<i>A</i> / MHz	1857.35494(28)	2380.92342(24)
<i>B</i> / MHz	722.78592(18)	619.03595(14)
<i>C</i> / MHz	605.95880(16)	564.49445(12)
Δ_J / kHz	0.0519(17)	0.02506(59)
Δ_{JK} / kHz	-0.0408(88)	0.1066(41)
Δ_K / kHz	0.507(14)	0.159(11)
δ_J / kHz	0.00651(92)	0.00422(26)
δ_K / kHz	0.263(30)	0.656(41)
χ_{aa} / MHz	23.9678(43)	-37.1858(47)
χ_{bb} / MHz	-58.6067(58)	14.7407(63)
χ_{cc} / MHz	34.6389(101)	22.4451(110)
$ \chi_{ab} $ / MHz	-33.938(72)	29.33(15)
$ \chi_{ac} $ / MHz	8.73(30)	-24.91(17)
$ \chi_{bc} $ / MHz	-21.957(96)	10.61(14)
N	776	705
σ / kHz	12.1	13.1

4.2.3 Conformer C

Even when conformers A and B (^{35}Cl and ^{37}Cl) were removed from the spectrum many transitions were still visible. However, the assignment of new species was more difficult for two reasons. First of all, the predictions for a plausible third conformer in section 4.1 suggested very low electric dipole moments ($\mu_a \sim 0.1 \text{ D} < \mu_b \sim 0.3 \text{ D} \sim \mu_c \sim 0.3 \text{ D}$). Second, the smallest component was in the a inertial axis, which usually gives rise to some recognizable spectral patterns. After successive attempts in which we scaled and varied the predicted rotational constants, finally we recognized in the spectrum several close lines made of one μ_b and one μ_c transitions in the region 12-14 GHz. We present two examples in Figure 4.11, like the pairs $4_{4,1} \leftarrow 3_{3,0} / 4_{4,1} \leftarrow 3_{3,1}$ and $5_{3,2} \leftarrow 4_{2,3} / 5_{3,3} \leftarrow 4_{2,3}$. Once a first set of lines was assigned new transitions were included sequentially in the fit, and the new species denoted enflurane C. Finally we observed 776 transitions, which were analysed similarly to conformers A and B. The resulting rotational parameters are shown in Table 4.5 and include the rotational and all quartic centrifugal distortion constants.

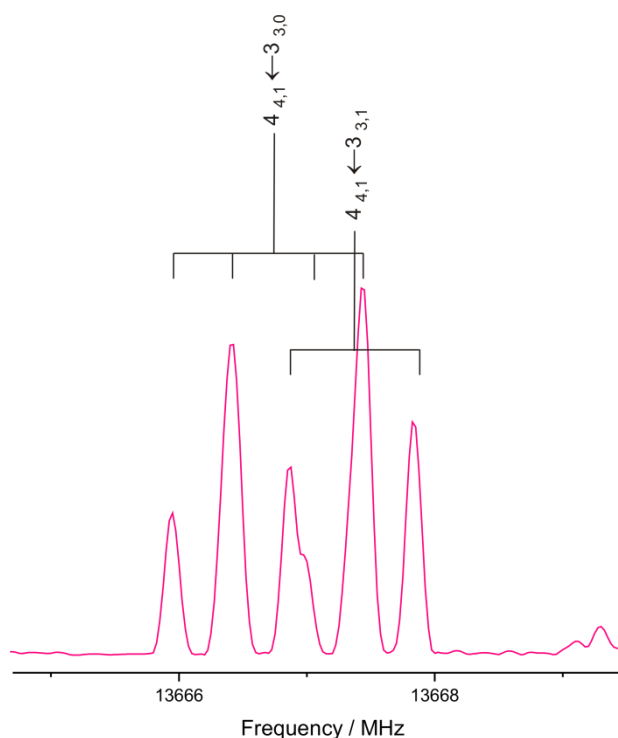


Figure 4.11. Example of rotational transitions of conformer C of enflurane.



For conformer C we could again determine all non-diagonal nuclear coupling elements, so the full tensor is presented in Table 4.5.

Following the assignment of conformers A, B and C, we searched for other different conformations, but no additional species were observed in the spectrum.

Table 4.5. Experimental results for conformer C

	³⁵ Cl-enflurane C	³⁷ Cl-enflurane C
A / MHz	1857.35494(28)	1830.71055(48)
B / MHz	722.78592(18)	714.22486(35)
C / MHz	605.95880(16)	597.21181(29)
Δ_J / kHz	0.0519(17)	0.0496(35)
Δ_{JK} / kHz	-0.0408(88)	-0.062(19)
Δ_K / kHz	0.507(14)	0.517(29)
δ_J / kHz	0.00651(92)	0.0061(20)
δ_K / kHz	0.263(30)	0.285(68)
χ_{aa} / MHz	23.9678(43)	18.2100(73)
χ_{bb} / MHz	-58.6067(58)	-45.3488(99)
χ_{cc} / MHz	34.6389(101)	27.1388(172)
$ \chi_{ab} $ / MHz	-33.938(72)	-27.67(14)
$ \chi_{ac} $ / MHz	8.73(30)	-7.41(55)
$ \chi_{bc} $ / MHz	-21.957(96)	-17.30(19)
N	776	447
σ / kHz	12.1	14.6

4.2.4 Isotopic species

The isotopic substitution of molecular atoms has a fundamental application in rotational spectroscopy: the structural determination. The rotational constants depend critically on the moments of inertia of the molecule, which are directly related to the atomic masses and the molecular geometry. The change of a single mass unit in any of



the molecular atoms represents a large change in the moments of inertia. This is why each isotopic species generate different rotational spectra, unlike in other techniques.

Generally, it is not necessary to prepare chemically new isotopologues. Organic molecules have some characteristic atoms with several isotopes in natural abundance, which generate isotopologues that give rise to different spectra. In our case carbon, oxygen and chlorine exhibit naturally two different isotopes that in principle could be detected by rotational spectroscopy. As we mentioned before the most notorious in enflurane is the chlorine atom, with two principal isotopes (^{35}Cl and ^{37}Cl). The natural abundances are 75.77% and 24.23% respectively [43], so the intensity of the rotational transitions of the ^{37}Cl isotopologues is remarkable and easily identifiable.

The natural abundance of ^{13}C is about 1%, so the rotational transition of the ^{13}C isotopologues would be ca. 100 times less intense than the rotational transitions of the parent species. These isotopologues can be detected under good circumstances, mostly depending on the number of species, fine and hyperfine effects and electric dipole moment. The natural abundance of ^{18}O is about 0.2%, so the parent transitions would be ca. 500 times more intense. For this reason, ^{18}O isotopologues are much more difficult to detect. The fluorine atoms contain a single isotope in natural abundance (^{19}F), while deuterium atoms have an abundance of 0.015%, which require the preparation of special chemical samples for the detection of the rotational spectra.

In the study of enflurane the isotopologues with ^{37}Cl were easily identifiable for the three conformers detected experimentally and are reported in previous sections. We thus focused on the detection of the weaker ^{13}C and ^{18}O species, which would provide accurate structural information for the molecule. Considering that there are several conformations in the molecule we initiated our search on the most intense conformer A. Structural predictions used preliminary structures reproducing the rotational constants. We assumed that the structure is practically invariant by the isotopic substitution, so the rotational constants will change by a mass effect. We similarly assume that the isotopic substitution does not produce significant changes in

the centrifugal distortion constants or the nuclear quadrupole coupling constants, so for the prediction (and later fitting) process, these parameters were fixed to the values of the parent species.

Using this procedure, we initially predicted the rotational transitions for the three distinct ^{13}C isotopologues in the most intense conformer enflurane A. The carbon atoms were labelled as in Figure 4.12.

Inspection of the spectrum revealed that all three ^{13}C isotopologues could be detected in the available spectrum. We show in Figure 4.12 an example of the rotational transition $5_{3,3} \leftarrow 4_{2,3}$. The analysis of these rotational spectra was similar to the parent species, but only the rotational constants were fitted. The results for the three ^{13}C species of enflurane A are shown in Table 4.6.

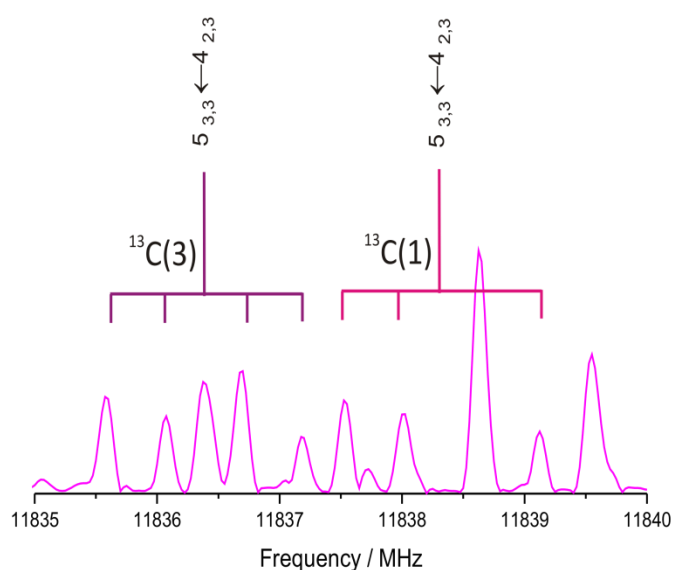


Figure 4.12. Examples of ^{13}C transitions observed in experimental spectrum.

We then proceeded to search for the ^{18}O species of enflurane A. Several intense transitions of the parent species were examined sequentially, but after a careful inspection of all the spectra available it was not possible to obtain a confident assignment for this species. The failure to detect the ^{18}O species must be attributed to the low intensity, due to its low natural abundance.



The isotopologues with ^{13}C were predicted just for the G- conformer, because it is the most intense conformer. The signals for other conformers spectra were not assigned.

Table 3.4. Experimental results for isotopic ^{13}C species of enflurane.

	$^{13}\text{C}(1)$	$^{13}\text{C}(2)$	$^{13}\text{C}(3)$
A / MHz	1655.15790(48)	1653.53728(10)	1656.0347(10)
B / MHz	738.05300(29)	740.63894(49)	736.65216(56)
C / MHz	680.46216(44)	682.84955(73)	679.4284(11)
Δ_J / kHz	[0.38870734]	[0.38870734]	[0.38870734]
Δ_{JK} / kHz	[2.063067779]	[2.063067779]	[2.063067779]
Δ_K / kHz	[2.285013634]	[2.285013634]	[2.285013634]
δ_J / kHz	[-0.128852666]	[-0.128852666]	[-0.128852666]
δ_K / kHz	[5.80020202]	[5.80020202]	[5.80020202]
L_J / mHz	[-0.062101768]	[-0.062101768]	[-0.062101768]
$ \chi_{ab} / \text{MHz}$	[35.413387474]	[35.413387474]	[35.413387474]
$ \chi_{ac} / \text{MHz}$	[0.0000]	[0.0000]	[0.0000]
$ \chi_{bc} / \text{MHz}$	[-13.652101114]	[-13.652101114]	[-13.652101114]
N	68	39	70
σ / kHz	13.6	15.6	12.9

The spectrum of ^{18}O was tried to be assigned by comparing the prediction to the experimental spectrum, but this work did not have success, because the rotational transition observed in the experimental spectrum had not enough intensity to be discernible from the noise signals.



4.2.5 Conformational assignment

The identification of the observed species in the spectrum relied on several arguments.

Initially we compared the experimental rotational constants with those predicted theoretically. For simplicity we compare in Table 4.7 our experimental results for the parent species (^{35}Cl) only with those of the MP2 calculation (6-311++G(2df,p) basis set). In order to quantify the discrepancies between the experiment and the predictions, we tabulate also the relative errors (defined as (experiment-theory)/theory). We should also note that the theoretical rotational parameters correspond to the equilibrium values (r_e), while the experimental results represent the ground-state (r_0) values. Despite those formal differences, the comparison is quantitatively meaningful.

The first observation is that the most intense experimental conformation (enflurane A) does not correspond to the global minimum, but to the second predicted species or *gauche* (G^+). This fact is unambiguous since there is a large difference in the rotational constants for the three observed conformations. As an example in conformer G- the discrepancy between theory and experiment for the A rotational constant is only 13 MHz of conformer A, while it is about 733 and 209 MHz for conformers B and C, respectively.

Using the same argument conformer B is clearly identified with the higher-energy conformer *trans* (T). Finally, conformer C identifies with the predicted global minimum, or conformer *gauche* (G^-)

An additional argument for this conformational assignment is the comparison of the nuclear quadrupole coupling constants. The coupling tensor is related to the electric field gradient at the quadrupolar nucleus created by the molecule. In consequence it is very sensitive to the electronic environment of the quadrupolar atom, and, in consequence, to the chemical bond. In our case the chlorine atom exhibits the same chemical bond in the three conformers, but the orientation of the principal inertial axes and the position of the chlorine atom with respect to those axes changes depending of

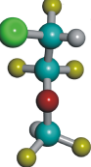
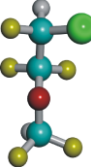
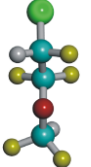


Elena Caballero Mancebo

Universidad de Valladolid

the conformation. For this reason, the nuclear quadrupole coupling parameters are a very sensitive indicator of conformation even when we consider the same chemical bond [45].

**Table 4.7.** Rotational parameters of enflurane (^{35}Cl parent species): Experiment vs. theory.

	Conformer G- 			Conformer G+ 			Conformer T 		
	Conformer C	Theory	Diff.	Conformer A	Theory	Diff.	Conformer B	Theory	Diff.
A / MHz	1857.35494(28)	1865.67	0.44	1656.134474(93)	1643.63	-0.76	2383.59171(19)	2389.65	0.25
B / MHz	722.78592(18)	727.54	0.65	740.909159(63)	749.86	1.19	631.455371(79)	636.08	0.73
C / MHz	605.95880(16)	609.31	0.55	683.074934(58)	694.49	1.64	574.955289(88)	578.37	0.59
Δ_J / kHz	0.0519(17)	0.04	-29	0.38871(39)	0.079	-329	0.02606(33)	0.02	-30
Δ_{JK} / kHz	-0.0408(88)	-0.02	-104	2.0630(13)	-0.094	2295	0.1053(16)	0.07	-50
Δ_K / kHz	0.507(14)	0.39	-30	2.2850(21)	0.351	-551	0.154(10)	0.18	14000
δ_J / kHz	0.00651(92)	0.01	34	-0.12885(11)	0.0084	1634	0.00462(14)	0.0038	-21
δ_K / kHz	0.263(30)	0.19	-38	5.8002(78)	0.473	-1126	0.632(19)	0.35	-80
L_J / mHz				-0.0621(41)					
χ_{aa} / MHz	23.9678(43)	21.98	-9.04	27.6750(27)	28.56	3.1	-46.9715(36)	-43.78	-7.3
χ_{bb} / MHz	-58.6067(58)	-54.37	-7.79	-61.5755(37)	-59.32	-3.8	18.4503(50)	16.58	-11
χ_{cc} / MHz	34.6389(101)	32.39	-6.94	33.9005(64)	30.76	-10	28.5211(86)	27.20	-4.9
$ \chi_{ab} / \text{MHz}$	33.938(72)	31.98	-6.12	-35.41(12)	-28.16	-25	37.61(16)	36.03	-4.4
$ \chi_{ac} / \text{MHz}$	8.73(30)	8.19	-6.59	[0.0000]	6.67	-	-31.36(20)	-28.88	-8.6
$ \chi_{bc} / \text{MHz}$	-21.957(96)	-19.92	-10.23	13.652(42)	15.80	14	13.742(28)	13.05	-5.3
$ \mu_a / \text{D}$		0.12			0.63			0.31	
$ \mu_b / \text{D}$		0.28			1.03			0.89	
$ \mu_c / \text{D}$		0.21			1.73			0.09	
$ \mu_{\text{TOT}} / \text{D}$		0.37			2.11			0.94	
ΔE^{MP2}		0.0			0.69			0.86	
$\Delta E^{\text{CCSD(T)}}$		0.0			0.27			1.19	

The column “Diff” indicates the relative error between the theoretical and experimental data. These differences have been calculated with the equation:

$$Diff = \frac{Theory - Experiment}{Theory} \cdot 100$$

The results of this calculation show that the discrepancy between theoretical and experimental data of rotational constants are small, so the assignment of the different conformers is correct. On the other hand, the values obtained for centrifugal distortion constants are too high. This is because the theoretical calculations follow a harmonic approximation that differs from the experiment, so the error is larger than in other parameters.

4.2.6 Structural determination

The enflurane structure was determined from the spectroscopic parameters of the most intense conformer G^- . As the rotational constants of four isotopologues of G^- conformer are known, this isotopic information produces structural determination through different methods. In this case, the substitution structure (r_s) and the effective structure (r_0) were determined.

4.2.6.1 Substitution structure (r_s):

This method is based in the Kraitchmann equations and generates the molecular structure by determining sequentially the atomic coordinates for each atom. For that, all atoms need to be substituted with a different isotopic species. In order to avoid a chemical synthesis usually we observe only those isotopic species that are detectable in natural abundance. For this reason a full substitution structure is generally not possible.



The structure generated by this method is an approximation to the equilibrium structure in which we assume similar contributions of the molecular vibrations to the moments of inertia. In consequence, the differences between the experimental moments of inertia of the parent and the isotopically substituted species tend to cancel approximately the vibrational contributions.

The substitution method is the most common method in rotational spectroscopy where the atomic coordinates are determined independently for each atom without any external data like ab initio calculations. On the other hand, this method presents some disadvantages:

- The Kraitchman equations generate absolute atomic coordinates, so a comparison with theoretical predictions is needed to determine the sign of these coordinates.
- The substitution method is not valid for atoms close to the inertial axes, because it produces large uncertainties and eventually complex atomic coordinates.

Table 4.8 shows a comparison between the results for the substitution coordinates in enflurane and the ab initio calculations. The substitution coordinates show a good correlation with the ab initio predictions, confirming the conformational assignment. In this calculation the coordinates predicted with a low magnitude or complex coordinates were fixed to zero. The errors in the atomic coordinates were calculated according to Costain's rule. The main problem of the substitution structure was the lack of experimental data for the ^{18}O isotopologue, so it was not possible to obtain the structure of the ether skeleton.

Table 4.8. Substitution coordinates of the G⁻ structure.

	Substitution coordinates ^a			Ab initio MP2/6-311++G(2df,p)		
	<i> a </i>	<i> b </i>	<i> c </i>	<i>a</i>	<i>b</i>	<i>c</i>
Cl	2.1741(7)	1.2080(13)	0.215(7)	-2.104	-1.256	0.245
C ₁	1.62939(93)	0.4400(34)	[0.000]	-1.639	0.413	-0.022
C ₂	0.086(18)	0.4879(38)	0.4929(31)	-0.195	0.503	-0.504
C ₃	1.98887 (77)	0.1590(97)	[0.000]	1.987	-0.060	0.078

^aPrincipal inertial axis denoted as *a*, *b*, *c*. ^bValues in square brackets constrained to zero. ^cErrors in parenthesis in units of the last digit, calculated as the sum of the standard errors and the Costain's estimates: $\Delta z = K/|z|$ ($K=0.15 \text{ \AA}$).

3.2.6.2 Effective structure (r_0):

The effective structure was determined using an iterative least-squares fit of the ground-state rotational constants for the different isotopic species observed. For this calculation we used the Kisiel program STRFIT [45]. Five structural parameters (angles and dihedrals) were selected as fitting parameters, including three valence angles ($\angle(\text{C}_1\text{-C}_2\text{-O})$, $\angle(\text{C}_2\text{-O-C}_3)$, $\angle(\text{Cl-C}_1\text{-C}_2)$) and two dihedrals ($\tau(\text{C}_1\text{-C}_2\text{-O-C}_3)$, $\tau(\text{Cl-C}_1\text{-C}_2\text{-O})$). The bond lengths were not determinable with our experimental dataset. The results of the fit are shown in table 4.9.

Table 4.9. Effective structure of the G⁻ conformer.

	r_0 Fit 1	<i>Ab initio</i> r_e
$r(\text{C}_1\text{-C}_2) / \text{Å}$		1.526
$r(\text{C}_2\text{-O}) / \text{Å}$		1.357
$r(\text{C}_3\text{-O}) / \text{Å}$		1.389
$r(\text{C}_1\text{-Cl}) / \text{Å}$		1.753
$r(\text{C}_1\text{-F}_1) / \text{Å}$		1.354
$r(\text{C}_2\text{-F}_2) / \text{Å}$		1.345
$r(\text{C}_2\text{-F}_3) / \text{Å}$		1.354
$r(\text{C}_3\text{-F}_4) / \text{Å}$		1.340
$r(\text{C}_3\text{-F}_5) / \text{Å}$		1.333
$\angle(\text{C}_1\text{-C}_2\text{-O})$	111.07(12)	110.2
$\angle(\text{C}_2\text{-O-C}_3)$	116.88(36)	115.9
$\angle(\text{Cl-C}_1\text{-C}_2)$	113.50(25)	110.8
$\angle(\text{C}_2\text{-C}_1\text{-F}_1)$		108.4
$\angle(\text{C}_1\text{-C}_2\text{-F}_2)$		109.5
$\angle(\text{C}_1\text{-C}_2\text{-F}_3)$		108.1
$\angle(\text{O-C}_3\text{-F}_4)$		109.1
$\angle(\text{O-C}_3\text{-F}_5)$		106.7
$\tau(\text{C}_1\text{-C}_2\text{-O-C}_3)$	172.39(54)	176.8
$\tau(\text{Cl-C}_1\text{-C}_2\text{-O})$	-63.38(97)	-60.7
$\tau(\text{F}_1\text{-C}_1\text{-C}_2\text{-O})$		60.9
$\tau(\text{F}_2\text{-C}_2\text{-O-C}_3)$		54.7
$\tau(\text{F}_3\text{-C}_2\text{-O-C}_3)$		-63.5
$\tau(\text{F}_4\text{-C}_3\text{-O-C}_2)$		-99.8
$\tau(\text{F}_5\text{-C}_3\text{-O-C}_2)$		143.6
$\tau(\text{H-C}_3\text{-O-C}_2)$		22.3

Due to the absence of experimental data for the ^{18}O isotopic species the structural information is limited. Nevertheless, some important parameters were calculated and the relevant conformational properties can be discussed.

5. Conclusions

The analysis of the rotational spectrum of enflurane in gas phase led to the identification of three different conformers, mostly differing in the orientation of the chlorine atom. The conformational assignment of two *gauche* (G^- , G^+) and one *trans* (T) species is consistent with the theoretical calculations, which predict these structures as the most stable. The rotational spectra were reproduced to experimental precision with a semi-rigid rotor Hamiltonian. The nuclear quadrupole coupling hyperfine effects caused by the chlorine nucleus were resolved for all rotational transitions and the full coupling tensor was determined.

The spectrum also let us to check the validity of the theoretical results provided by the different methods used during this project. After the reoptimization of the starting structures obtained with MM, six most stable structures were calculated using DFT and MP2 methods, all of them with a low and very close electronic energy (less than 1.4 kJ mol^{-1}). We observed that the molecular orbital calculations are able to reproduce satisfactorily the rotational constants of enflurane in gas phase (to ca. 1.6%). Each of the three chlorine *gauche* or *trans* orientations exhibits two possibilities for the terminal difluoromethyl group, with C-H bond dihedrals ca. ± 20 degrees away from the *cis* arrangement. The MP2 electronic energies are very close for each member or the pair. However, only a single species is observed for each chlorine orientation. Due to the use of a supersonic expansion to obtain the experimental spectrum, most plausibly the higher energy forms could relax collisionally in the jet. The calculation of Gibbs free energies, which include entropic factors, gives a different perspective since the non-observed conformations are now predicted much higher in energy ($7\text{-}12 \text{ kJ mol}^{-1}$) and might be depopulated.

In order to further verify the conformational energies the MP2 predictions were supplemented with additional coupled-cluster CCSD(T) calculations (at the MP2 geometries). However, the ordering of the CCSD(T) electronic energies is similar to



MP2. In any case, the three experimentally detected conformations correspond to the lower energy conformations predicted theoretically with both MP2 and CCSD(T), so the agreement between observations and predictions is satisfactory.

The analysis of the spectrum for the parent species was extended to four monosubstituted species in natural abundance of the most intense conformer G^- . Apart from the relatively intense ^{37}Cl species, we assigned the weak signals from three ^{13}C independent spectra. In conformers G^+ and T only the ^{37}Cl isotopologues were detectable, due to its lower intensity. The ^{18}O species could not be detected despite a careful search and the good sensitivity of the instrument, as the total intensity is divided into no less than 9 different species and each transition is split by the hyperfine effects. Rotational parameters were accurately determined for all isotopologues.

Additionally, the structural analysis produced substitution and effective structures that were compared to the equilibrium ab initio predictions, showing a good correlation between the experimental and theoretical data.

We solved the structural uncertainties of previous investigations, providing a definitive picture of the molecule. We confirmed that the ether C-O-C-C skeleton is *trans* in the gas-phase, as reported in the GED work [10] and previous studies on related molecules, like . The IR spectra in CCl_4 and cryogenic matrix are also consistent with this observation [11]. The suggestions of the NMR study [13] that the terminal carbon is out of the C-C-O plane are not justifiable, at least in the gas-phase. The preferred orientation of the chlorine atom in enflurane is definitively attributed to the *gauche* species, not the *trans* claimed in the GED [10] and IR [11] studies, who confused the global minimum. The near isoenergetic situation of the most stable conformations of enflurane is at the origin of this problem, which is difficult to solve with theoretical methods. Experimental information on the conformational energies would require relative intensity measurements of the rotational transitions, which were not done in this work. The claim of the IR work that four conformers had been detected should be taken with caution. The initial conformational search of



Oberhammer, despite apparently extensive, missed several conformations and is completed in our work.

The origin of the structural preferences of enflurane has been discussed by Oberhammer and Zeegers-Huyskens in terms of hyperconjugative interactions [10, 11].

In conclusion, this work has presented a detailed description of the structural properties of enflurane, setting the condition for future characterizations of intermolecular complexes where enflurane is present. Microsolvation and dimerization studies have particular biological interest.



6. References

- [1] a) Urban, B. W.; Barann, M. (Eds.), *Molecular and Basic Mechanisms of Anesthesia*; Pabst Science Publishers: Lengerich, 2002. b) Franks, N. P.; Lieb, W. R., *Nature* 1994, 367, 607
- [2] a) Nury, H.; Van Renterghem, C.; Weng, Y.; Tran, A.; Baaden, M.; Dufresne, V.; Changeux, J. P.; Sonner, J. M.; Delarue, M.; Corringer, P. J. *Nature* 2011, 469, 428. b) Bocquet, N.; Nury, H.; Baaden, M.; Le Poupon, C.; Changeux, J. P.; Delarue, M.; Corringer, P. J. *Nature* 2009, 457, 111.
- [3] Schermann, J. P., *Spectroscopy and modelling of biomolecular building blocks*; first edition ed.; Elsevier: Amsterdam, 2008
- [4] Caminati W., "Microwave Spectroscopy of Large Molecules and Molecular Complexes", in *Handbook of High Resolution Spectroscopy* (Ed.: M. Quack, F. Merkt), vol. II, pp. 829-852, Wiley: Chichester, 2010.
- [5] Grabow J.-U., "Fourier Transform Microwave Spectroscopy Measurement and Instrumentation" in *Handbook of High Resolution Spectroscopy* (Ed.: M. Quack, F. Merkt), vol. II, pp. 723-800, Wiley: Chichester, 2010.
- [6] Evers, A. S., Crowder, C. M. and Balsler, J. R., in *Goodman & Gilman's The Pharmacological Basis of Therapeutics*, (Eds. Brunton, L. L.; Lazo, S. and Parker, K. L.), McGraw-Hill, New York, 2006, 11th. edn, ch. 13.
- [7] Lesarri, A., Vega-Toribio, A., Suenram, R. D., Brugh, D. J., Grabow, J.-U., *Phys. Chem. Chem. Phys.*, 2010, 12, 9624.
- [8] Lesarri, A., Vega-Toribio, A., Suenram, R. D., Brugh, D. J., Nori-Shargh, D., Boggs, J. E., Grabow, J.-U., *Phys. Chem. Chem. Phys.*, 2011, 13, 6610.
- [9] Suenram, R. D., Shipman, S. T., Pate, B. H., Brown, G. G., 66th *OSU Int. Symp. Mol. Spectrosc.*, Columbus (OH), Comm. RH06, 2008.
- [10] Pfeiffer, A., Mack, H.-G., Oberhammer, H., *J. Am. Chem. Soc.*, 1998, 120, 6384
- [11] a) Michalska, D., Bieńko, D. C., Czarnik-Matuszewicz, B., Wierzejewska, M., Sandorfy, C., & Zeegers-Huyskens, T. *Theoretical and experimental studies of enflurane. Infrared spectra in solution, in low-temperature argon matrix and blue shifts resulting from dimerization*. *The Journal of Physical Chemistry. B*, 2007, 111(42), 12228–38. doi:10.1021/jp073772r; b)
- [12] Zhao, C., Polavarapu, P. L., Grosenick, H., Schurig, V., 2000, *J. Mol. Struct.*, 2000, 550-551, 105.
- [13] Balonga, P. E., Kowaleski, W. J., Contreras, R. H., *Spectrochim. Acta A*, 1988, 44A, 819.
- [14] Zierkiewicz, W., Michalska, D., & Zeegers-Huyskens, T., *J. Mol. Model.*, 2010 19(3), 1399.
- [15] a) Zierkiewicz, W., Zalesny, R., & Hobza, P. (2013). On the nature of unusual intensity changes in the infrared spectra of the enfluraneacetone complexes. *Physical*



Chemistry Chemical Physics, 15(16), 6001. b) Zierkiewicz, W., Czarnik-Matusiewicz, B., & Michalska, D. (2011). Blue Shifts and Unusual Intensity Changes in the Infrared Spectra of the Enflurane...Acetone Complexes: Spectroscopic and Theoretical Studies. *The Journal of Physical Chemistry A*, 115(41), 11362.

[16] Zierkiewicz, W., Wieczorek, R., Hobza, P., & Michalska, D. (2011). Halogen bonded complexes between volatile anaesthetics (chloroform, halothane, enflurane, isoflurane) and formaldehyde: a theoretical study. *Physical Chemistry Chemical Physics*, 13(11), 5105–5113. doi:10.1039/C0CP02085K

[17] Zierkiewicz, W. (2010). Modelling of interactions between volatile anaesthetics (halothane, enflurane) and aromatic compounds, ab initio study. *Chemical Physics*, 373(3), 243–250. doi:10.1016/j.chemphys.2010.05.017

[18] Gordy, W., Cook, R. L., *Microwave Molecular Spectra*, Wiley, New York, 1984.

[19] Kroto, H. W., *Molecular Rotation Spectra*, Dover Phoenix Editions, 2003.

[20] Brown, J. M., Carrington, A., *Rotational Spectroscopy of Diatomic Molecules*, Cambridge Univ. Press, Cambridge, 2003.

[21] Jensen, F., *Introduction to Computational Chemistry*, Wiley, Chichester, 2007.

[22] Pickett, H. M., *J. Molec. Spectroscopy*, 1991, 148, 371.

[23] Molecular Spectroscopy Group, Jet Propulsion Laboratory (California Institute of Technology): <http://spec.jpl.nasa.gov/>

[24] Watson, J. K. in *Vibrational Spectra and Structure*, ed. J. R. Durig, Elsevier, Amsterdam, 1977, vol. 6, pp. 1–89.

[25] HyperChem Professional 8.0, Hypercube, Inc., 2010.

[26] MacroModel, version 9.2, Schrödinger, LLC, New York, NY, 2012.

[27] Halgren, T. A., *J. Comp. Chem.* 1999, 20, 720-729. b) Halgren, T. A., *J. Comp. Chem.* 1999, 20, 730-748.

[28] Ostlund, N. S., Szabo, A., *Modern Quantum Chemistry: Introduction to advanced electronic structure theory*, McMillan, New York, 1982.

[29] Cremer, D., *Wiley Interdisciplinary Reviews: Computational Molecular Science*, 2011, 1, 509.

[30] Gaussian 09, Frisch, M. J.; Trucks, G. W.; Schlegel, H. B.; Scuseria, G. E.; Robb, M. A.; Cheeseman, J. R.; Scalmani, G.; Barone, V.; Mennucci, B.; Petersson, G. A.; Nakatsuji, H.; Caricato, M.; Li, X.; Hratchian, H. P.; Izmaylov, A. F.; Bloino, J.; Zheng, G.; Sonnenberg, J. L.; Hada, M.; Ehara, M.; Toyota, K.; Fukuda, R.; Hasegawa, J.; Ishida, M.; Nakajima, T.; Honda, Y.; Kitao, O.; Nakai, H.; Vreven, T.; Montgomery, J. A., Jr.; Peralta, J. E.; Ogliaro, F.; Bearpark, M.; Heyd, J. J.; Brothers, E.; Kudin, K. N.; Staroverov, V. N.; Kobayashi, R.; Normand, J.; Raghavachari, K.; Rendell, A.; Burant, J. C.; Iyengar, S. S.; Tomasi, J.; Cossi, M.; Rega, N.; Millam, N. J.; Klene, M.; Knox, J. E.; Cross, J. B.; Bakken, V.; Adamo, C.; Jaramillo, J.; Gomperts, R.; Stratmann, R. E.; Yazyev, O.; Austin, A. J.; Cammi, R.; Pomelli, C.; Ochterski, J. W.; Martin, R. L.; Morokuma, K.; Zakrzewski, V. G.; Voth, G. A.; Salvador, P.; Dannenberg, J. J.; Dapprich, S.; Daniels, A. D.; Farkas, Ö.



Foresman, J. B.; Ortiz, J. V.; Cioslowski, J.; Fox, D. J. Gaussian, Inc., Wallingford CT, 2009.

[31] Raghavachari, K, Trucks, G. W., Pople, J. A., Head-Gordon, M. Chem. Phys. Lett. 1989, 157, 479

[32] a) Koch, W., Holthausen, M. C., A Chemist's Guide to DFT, VCH, Weinheim, 1999. b) Kohn, W., Becke, A. D. Parr., R. G., J. Phys. Chem. 100, 12974-12980, 1996.

[33] Becke, A. D. J. Chem. Phys. 1993, 98, 5648.

[34] Zhao, Y., Truhlar. D. G. Acc. Chem. Res., 41, 157-167, 2008.

[35] Raghavachari, K., Binkley, J. S., Seeger, R., Pople, J. A., J. Chem. Phys., 1980, 72, 650.

[36] Elliel, E. L., Conformational Analysis, ACS, Bocaraton, 1981

[37] Godfrey, P. D.; Brown, R. D.; Rodgers, F. M. J. Mol. Struct. 1996, 376, 65.

[38] Blanco, S., López, J. C., Mata, S., & Alonso, J. L.. *Conformations of γ -aminobutyric acid (GABA): the role of the $n \rightarrow \pi^*$ interaction*. Angewandte Chemie (International Ed. in English), 2010, 49(48), 9187–92.

[39] R. D. Suenram, D. J. Brugh, F. J. Lovas and C. Chu, 54th OSU Int. Symp. on Mol. Spectrosc. (ISMS), Columbus (OH), 1999, Comm. RB07.

[40] Balle, T. J.; Flygare, W. H. Rev. Sci. Instrum. 1981, 52, 33

[41] Vega-Toribio, A, Lesarri, A., Suenram, R. D., Grabow, J.-U., 64th OSU Int. Symp. on Mol. Spectrosc. (ISMS), Columbus (OH), 2009, Comm. MH07.

[42] Shipman, S. T., Pate, B. H., *New Techniques in Microwave Spectroscopy*, in *Handbook of High Resolution Spectroscopy* (Ed.: M. Quack, F. Merkt), vol. II, pp. 801-828, Wiley: Chichester, 2010.

[43] *Quantities, Units and Symbols in Physical Chemistry, IUPAC Green Book*, third edition (E.R. Cohen, T. Cvitas, J.G. Frey, B. Holmström, K. Kuchitsu, R. Marquardt, I. Mills, F. Pavese, M. Quack, J. Stohner, H.L. Strauss, M. Takami, and A.J. Thor, IUPAC & RSC Publishing, Cambridge, 2008.

[44] Z. Kisiel, AABS, available at: <http://info.ifpan.edu.pl/~kisiel/prospe.htm>

[45] Écija, P., Cocinero, E. J., Lesarri, A., Millán, J., Basterretxea, F. J., Fernández, J. A., Castaño, F., J. Chem. Phys. 2011, 134, 164311.

7. Annexes

Table 7.1. Summary of ^{35}Cl transitions observed for isotopic species of conformer 1.

J'	K_{-1}'	K_{+1}'	F'	J''	K_{-1}''	K_{+1}''	F''	obs. ^a	$\text{o.} - \text{c.}^{\text{b}}$
7	2	6	8	7	1	6	8	2057,8643	0.0038
7	2	6	7	7	1	6	7	2060,2478	0.0016
7	2	6	8	7	1	6	7	2061,1201	-0.0024
7	2	6	9	7	1	6	9	2069,535	0.0121
7	2	6	6	7	1	6	6	2071,8966	0.0100
4	0	4	3	3	1	2	2	4551,4286	-0.0008
6	3	4	8	6	2	4	7	4581,425	0.0072
6	3	4	5	6	2	4	6	4583,2553	0.0001
4	3	2	4	4	2	2	5	4685,8065	0.0017
4	3	2	5	4	2	2	4	4686,9339	-0.0041
4	3	1	6	4	2	2	5	4687,0252	0.0001
4	3	1	5	4	2	2	4	4687,4085	-0.0070
4	3	2	4	4	2	2	4	4687,8957	-0.0024
4	3	1	4	4	2	2	4	4688,1666	-0.0070
4	3	2	3	4	2	2	4	4689,3798	0.0002
3	3	0	4	3	2	2	3	4716,5307	-0.0472
3	3	0	4	3	2	2	5	4716,5307	-0.0520
3	3	1	2	3	2	1	2	4717,0158	-0.0045
3	3	0	3	3	2	2	2	4720,3991	0.0001
3	3	0	3	3	2	2	3	4720,47	-0.0096
3	3	1	5	3	2	2	5	4724,8732	-0.0141
3	3	0	5	3	2	2	5	4724,9538	-0.0035
4	3	2	5	4	2	3	5	4726,351	-0.0014
4	3	1	5	4	2	3	5	4726,8272	-0.0027
4	3	2	5	4	2	3	4	4727,2945	-0.0112
4	3	1	4	4	2	3	5	4727,5814	-0.0066
4	3	1	5	4	2	3	4	4727,7806	-0.0027
4	3	2	4	4	2	3	4	4728,2602	-0.0056
4	3	1	4	4	2	3	4	4728,5368	-0.0045
6	1	5	5	5	2	3	4	6187,8773	-0.0002
7	0	7	8	6	0	6	7	9832,9968	-0.0036
7	0	7	7	6	0	6	6	9833,38	-0.0028
7	0	7	9	6	0	6	8	9834,8795	-0.0014
7	1	7	6	6	0	6	5	9835,2665	-0.0031
8	7	0	6	7	6	2	6	12266,0374	0.0203
8	0	1	6	7	6	1	6	12266,0374	0.0203
8	0	9	8	8	1	8	7	12274,9587	-0.0012
8	0	9	9	8	1	8	8	12277,5157	-0.0037



8	0	9	11	8	1	8	10	12275,5265	-0.0011
8	4	9	10	8	1	8	9	12278,0672	-0.0039
8	4	1	5	3	3	0	5	12295,5378	0.0114
7	4	1	5	3	3	1	5	12295,5378	-0.0586
7	4	1	4	3	3	0	3	12303,3362	0.0310
7	0	1	4	3	3	1	3	12303,3362	-0.0468
11	0	11	11	10	0	1	10	15286,7268	-0.0029
6	0	11	10	10	0	1	10	15287,8568	0.0000
6	1	11	13	10	0	1	10	15287,7948	0.0003
6	1	8	8	8	0	8	7	15309,5946	-0.0288
6	1	8	11	8	0	8	10	15312,445	-0.0278
6	1	8	9	8	0	8	8	15326,9975	-0.0276
6	2	8	10	8	0	8	9	15329,8649	-0.0294
6	2	7	11	8	1	7	10	15375,1149	0.0051
6	2	7	8	8	1	7	7	15375,278	0.0044
6	2	7	10	8	1	7	9	15375,9195	0.0051
6	4	7	9	8	1	7	8	15376,0771	0.0046
9	4	5	9	7	3	4	8	17984,5932	0.0006
9	4	5	8	7	3	4	7	17985,1041	0.0007
9	4	5	10	7	3	4	9	17986,6986	0.0049
9	4	5	7	7	3	4	6	17987,2088	0.0040
9	4	4	9	7	3	5	8	18001,6771	0.0009
8	2	9	10	10	1	9	9	18421,5959	0.0094
8	2	9	13	10	1	9	12	18422,0497	0.0092
8	2	9	11	10	1	9	10	18426,2435	0.0101
8	5	9	12	10	1	9	11	18426,6952	0.0104
8	5	2	8	6	4	2	7	18462,6652	-0.0202
13	5	2	8	6	4	3	7	18462,806	0.0358
13	5	3	7	6	4	3	7	18463,0878	-0.0499
13	5	2	7	6	4	3	6	18463,2373	0.0425
13	5	3	9	6	4	2	8	18464,2986	-0.0236
13	3	11	15	12	3	1	10	18547,3724	0.0109
13	3	11	14	12	3	1	10	18547,3865	0.0053
13	3	11	12	12	3	1	10	18547,4288	0.0105
11	5	11	13	12	3	1	10	18547,4534	0.0052
11	5	9	12	12	5	8	11	18553,4077	-0.0055
11	5	9	15	12	5	8	14	18553,444	-0.0055
11	5	9	13	12	5	8	12	18554,0958	-0.0096
7	5	8	12	12	5	7	11	18554,3157	-0.0064
7	5	8	15	12	5	7	14	18554,3543	-0.0060
7	5	8	13	12	5	7	12	18555,024	-0.0087
7	4	8	14	12	5	7	13	18555,0507	-0.0098
7	4	10	12	12	4	9	11	18570,5586	0.0050

^aFrecuencia observada ^b(Frecuencia observada – Frecuencia calculada)

**Table 7.2.** Summary of ^{37}Cl transitions observed for isotopic species of conformer 1.

J'	K_{-1}'	K_{+1}'	F'	J''	K_{-1}''	K_{+1}''	F''	obs. ^a	o. - c. ^b
1	1	1	3	0	0	0	2	2314,9209	0.0034
1	1	1	1	0	0	0	2	2324,429	-0.0018
7	2	5	7	7	1	6	7	2359,8287	0.0018
7	2	5	9	7	1	6	9	2361,5602	0.0069
1	1	0	1	0	0	0	2	2364,6454	0.0002
1	1	0	3	0	0	0	2	2369,9047	0.0007
1	1	0	2	0	0	0	2	2376,6665	-0.0019
5	2	4	7	5	1	4	6	2379,7489	0.0161
5	2	4	6	5	1	4	6	2382,5614	0.0013
5	2	4	5	5	1	4	5	2385,397	0.0024
5	2	3	4	4	3	1	3	2390,7499	-0.0010
2	2	1	2	2	1	1	1	2741,2463	0.0001
2	1	2	1	1	1	1	1	2741,4855	-0.0015
2	2	0	2	2	1	1	1	2744,0547	-0.0017
2	1	2	2	1	1	1	3	2744,3004	-0.0070
2	1	2	4	1	1	1	3	2746,1727	0.0005
2	2	1	1	2	1	1	1	2746,616	0.0009
2	2	0	1	2	1	1	1	2748,805	0.0119
2	1	2	3	1	1	1	2	2751,4476	0.0001
2	1	2	2	1	1	1	2	2756,3004	-0.0009
2	0	2	2	1	0	1	2	2798,5089	-0.0021
2	0	2	3	1	0	1	2	2801,8072	-0.0018
2	0	2	4	1	0	1	3	2802,3674	-0.0013
2	0	2	1	1	0	1	1	2803,2895	-0.0034
2	0	2	3	1	0	1	3	2807,0356	-0.0017
2	0	2	2	1	0	1	1	2807,9909	-0.0042
2	1	1	2	1	1	0	2	2858,7253	0.0058
6	2	4	6	5	3	3	5	3871,4813	-0.0026
6	2	4	7	5	3	3	6	3873,1571	0.0023
8	2	7	7	8	1	8	7	3909,4166	0.0000
8	2	7	10	8	1	8 1	10	3911,165	0.0070
8	2	7	8	8	1	8	8	3918,7755	0.0101
8	2	7	9	8	1	8	9	3920,3798	0.0045
10	3	8	11	10	2	8 1	11	3932,9738	0.0049
10	3	8	10	10	2	8 1	10	3934,0981	0.0006
10	3	8	12	10	2	8 1	12	3940,7225	0.0013
10	3	8	9	10	2	8	9	3941,8246	0.0004
7	2	5	6	7	1	7	6	3979,7166	0.0116
7	2	5	9	7	1	7	9	3982,9776	0.0022
7	2	5	7	7	1	7	7	3995,692	0.0023
7	2	5	8	7	1	7	8	3998,9481	0.0010
10	3	7	11	10	2	8 1	11	4064,7225	-0.0096



3	1	3	4	2	1	2	4	4112,6254	-0.0011
3	1	3	2	2	1	2	1	4116,032	0.0014
3	1	3	3	2	1	2	2	4117,1178	0.0001
6	1	6	7	5	1	5	7	8214,2759	-0.0414
6	1	6	6	5	1	5	5	8219,4595	0.0020
6	1	6	8	5	1	5	7	8219,8638	0.0010
4	2	3	4	3	1	2	4	8243,2764	-0.0069
4	2	3	5	3	1	2	4	8244,0007	0.0001
4	2	3	3	3	1	2	3	8247,5205	0.0079
4	2	3	4	3	1	2	3	8249,4306	0.0003
4	2	3	6	3	1	2	5	8255,1405	-0.0003
4	2	3	5	3	1	2	5	8257,136	-0.0053
4	2	3	3	3	1	2	2	8260,5796	-0.0010
4	2	2	4	3	1	2	4	8284,9371	-0.0013
4	2	2	5	3	1	2	4	8286,5678	-0.0007
4	2	2	4	3	1	2	3	8291,0865	0.0010
4	2	2	6	3	1	2	5	8295,0982	0.0009
6	0	6	7	5	0	5	6	8324,6063	-0.0024
6	0	6	6	5	0	5	5	8325,0185	0.0010
6	0	6	8	5	0	5	7	8326,0887	0.0021
6	0	6	5	5	0	5	4	8326,4927	0.0042
9	1	9	10	8	2	7	9	8375,1635	-0.0109
9	1	9	9	8	2	7	8	8376,7126	-0.0110
9	1	9	11	8	2	7	10	8384,7608	-0.0001
9	3	6	11	8	3	5	10	12687,1807	0.0075
9	3	6	9	8	3	5	8	12688,1752	0.0363
9	3	6	10	8	3	5	9	12688,1752	-0.0202
9	1	8	10	8	1	7	9	12789,122	-0.0287
9	1	8	9	8	1	7	8	12789,5035	-0.0170
9	1	8	11	8	1	7	10	12790,0638	0.0014
9	1	8	8	8	1	7	7	12790,4194	-0.0071
9	2	7	11	8	2	6	10	12827,0047	0.0012
6	5	2	7	5	4	1	6	16866,9274	-0.0231
6	5	2	6	5	4	1	5	16867,0234	-0.0441
6	5	1	6	5	4	1	5	16867,0234	-0.0446
6	5	2	6	5	4	2	5	16867,0234	-0.0621
6	5	1	6	5	4	2	5	16867,0234	-0.0625
6	5	2	8	5	4	1	7	16867,9612	-0.0320
6	5	1	8	5	4	2	7	16867,9612	-0.0494
6	5	2	5	5	4	2	4	16868,08	-0.0466
8	4	4	9	7	3	4	8	17780,2543	-0.0432
8	4	4	10	7	3	4	9	17781,8661	-0.0316
8	4	5	9	7	3	5	8	17796,3176	-0.0393

^aFrecuencia observada ^b(Frecuencia observada – Frecuencia calculada)

**Table 7.3.** Summary of ^{35}Cl transitions observed for isotopic species of conformer 2.

J'	K_{-1}'	K_{+1}'	F'	J''	K_{-1}''	K_{+1}''	F''	obs. ^a	$\text{o.} - \text{c.}^{\text{b}}$
5	1	4	5	5	0	5	5	2242,0643	0.0018
5	1	4	6	5	0	5	6	2242,8524	0.0027
2	1	2	3	1	1	1	2	2347,7091	0.0006
2	1	2	2	1	1	1	2	2352,8631	0.0065
2	1	2	4	1	1	1	3	2359,3308	0.0015
2	1	2	1	1	1	1	2	2360,002	0.0574
2	1	2	2	1	1	1	1	2361,2652	-0.0044
2	1	2	1	1	1	1	1	2368,3564	-0.0012
2	0	2	2	1	0	1	1	2400,0035	-0.0461
2	0	2	3	1	0	1	3	2400,8504	0.0049
2	0	2	1	1	0	1	1	2411,8148	0.0005
2	0	2	4	1	0	1	3	2412,5039	-0.0016
2	0	2	3	1	0	1	2	2412,6161	0.0010
2	0	2	2	1	0	1	2	2421,1671	-0.0016
6	1	5	8	6	0	6	8	2444,6378	-0.0006
6	1	5	5	6	0	6	5	2444,7017	-0.0192
6	1	5	6	6	0	6	6	2446,4628	-0.0004
6	1	5	7	6	0	6	7	2447,1624	0.0000
2	1	1	3	1	1	0	2	2460,3732	0.0063
2	1	1	2	1	1	0	2	2463,6357	0.0016
2	1	1	3	1	1	0	3	2467,5822	0.0023
1	1	1	2	0	0	0	2	2962,0963	0.0000
8	1	7	7	8	0	8	7	2999,5675	0.0010
8	1	7	10	8	0	8	10	2999,9997	0.0484
3	1	3	3	2	0	2	2	5228,3968	-0.0005
3	1	3	5	2	0	2	4	5230,6272	0.0002
3	1	3	4	2	0	2	3	5232,2103	-0.0011
3	1	3	3	2	0	2	3	5236,9485	-0.0024
3	1	3	2	2	0	2	2	5238,4493	-0.0023
2	2	0	1	2	1	1	1	5241,2944	0.0018
2	2	0	1	2	1	1	2	5246,0226	0.0004
3	1	3	2	2	0	2	3	5247,0036	-0.0016
2	2	1	4	2	1	1	4	5251,771	-0.0028
2	2	0	2	2	1	1	1	5253,0286	-0.0020
2	2	0	4	2	1	1	4	5253,1109	0.0012
2	2	1	2	2	1	1	2	5256,3836	-0.0296
2	2	0	4	2	1	1	3	5257,6437	-0.0014
8	1	7	8	7	2	6	7	5277,688	-0.0005
8	1	7	9	7	2	6	8	5277,8603	-0.0018
8	1	7	10	7	2	6	9	5278,6202	-0.0007
8	1	7	7	7	2	6	6	5278,6988	0.0027



2	2	1	1	2	1	2	1	5407,1005	0.0008
2	2	1	1	2	1	2	2	5414,186	-0.0016
2	2	1	2	2	1	2	1	5418,8043	0.0009
2	2	1	4	2	1	2	4	5420,5516	0.0002
2	2	1	2	2	1	2	2	5425,8899	-0.0013
2	2	1	4	2	1	2	3	5427,6649	-0.0034
2	2	1	2	2	1	2	3	5431,0374	-0.0020
2	2	1	3	2	1	2	4	5432,316	-0.0037
2	2	1	3	2	1	2	2	5434,2864	-0.0022
2	2	1	3	2	1	2	3	5439,4345	-0.0022
3	2	2	2	3	1	3	2	5503,484	-0.0006
3	2	2	3	3	1	3	2	5503,6214	-0.0003
5	2	3	6	4	2	2	6	6049,9998	0.0096
5	2	3	6	4	2	2	5	6054,4263	0.0000
5	2	3	5	4	2	2	4	6055,4634	0.0011
5	2	3	7	4	2	2	6	6056,9013	0.0002
5	2	3	4	4	2	2	3	6056,982	-0.0076
7	2	6	6	7	1	7	6	6145,1971	0.0002
7	2	6	9	7	1	7	9	6146,0082	-0.0006
7	2	6	7	7	1	7	7	6148,5317	0.0000
7	2	6	8	7	1	7	8	6149,0791	-0.0004
5	1	4	6	4	1	3	6	6158,3251	-0.0001
5	1	4	5	4	1	3	4	6166,6293	0.0024
8	2	6	10	7	1	7	9	16053,7098	-0.0355
8	2	6	8	7	1	7	7	16056,0155	-0.0334
8	2	6	9	7	1	7	8	16056,9642	-0.0125
6	3	4	6	5	2	3	5	16112,6555	-0.0172
6	3	4	7	5	2	3	6	16114,0173	-0.0125
6	3	3	7	5	2	4	6	16162,637	-0.0192
4	4	1	3	3	3	0	3	17273,8113	-0.0220
4	4	1	4	3	3	0	4	17283,3452	-0.0264
4	4	0	4	3	3	0	4	17283,3452	-0.0267
4	4	1	4	3	3	1	4	17283,3452	-0.0466
7	3	5	6	6	2	4	5	17287,0342	-0.0301
7	3	5	9	6	2	4	8	17287,6418	-0.0343
4	4	1	3	3	3	0	2	17288,4798	-0.0031
4	4	0	3	3	3	0	2	17288,4798	-0.0033
4	4	1	3	3	3	1	2	17288,4798	-0.0228
4	4	0	3	3	3	1	2	17288,4798	-0.0230
4	4	1	5	3	3	0	4	17289,1523	-0.0065
7	3	4	9	6	2	5	8	17384,7448	0.0415
7	3	4	8	6	2	5	7	17387,1646	-0.0312
9	2	7	10	8	1	8	9	17637,7755	-0.0509

^aFrecuencia observada ^b(Frecuencia observada – Frecuencia calculada)

Table 7.4. Summary of ^{37}Cl transitions observed for isotopic species of conformer 2.

J'	K_{-1}'	K_{+1}'	F'	J''	K_{-1}''	K_{+1}''	F''	obs. ^a	$\text{o.} - \text{c.}^{\text{b}}$
2	0	2	4	1	0	1	3	2366,626	0.0002
2	0	2	3	1	0	1	2	2366,7016	0.0061
2	0	2	2	1	0	1	2	2373,4454	-0.0012
2	1	1	3	1	1	0	2	2414,5108	-0.0012
2	1	1	4	1	1	0	3	2423,8041	-0.0060
6	1	5	8	6	0	6	8	2427,9382	0.0010
6	1	5	7	6	0	6	7	2429,7689	-0.0168
7	1	6	6	7	0	7	6	2668,7597	0.0015
7	1	6	9	7	0	7	9	2669,1048	0.0009
7	1	6	7	7	0	7	7	2670,4704	0.0009
7	1	6	8	7	0	7	8	2670,792	-0.0320
1	1	1	1	0	0	0	2	2941,57	-0.0032
1	1	1	3	0	0	0	2	2944,6594	0.0008
1	1	1	2	0	0	0	2	2948,2712	-0.0012
8	1	7	7	8	0	8	7	2959,3938	0.0004
8	1	7	10	8	0	8	10	2959,6891	0.0003
3	1	3	4	2	1	2	4	3461,1239	-0.0006
6	2	4	5	6	1	5	5	4890,339	-0.0023
6	2	4	8	6	1	5	8	4890,6873	-0.0008
6	2	4	6	6	1	5	6	4891,6836	-0.0017
6	2	4	7	6	1	5	7	4891,9798	-0.0015
6	2	4	6	6	1	5	7	4893,5418	0.0409
6	2	4	5	6	1	5	6	4898,096	-0.0061
5	2	4	6	5	1	4	6	4964,7664	0.0111
5	2	3	6	5	1	4	7	5000,8604	-0.0062
5	2	3	4	5	1	4	4	5005,6326	-0.0014
5	2	3	7	5	1	4	7	5006,2693	-0.0004
5	2	3	5	5	1	4	5	5007,7187	-0.0006
5	2	3	6	5	1	4	6	5008,2565	-0.0008
9	1	8	9	8	2	7	8	6441,0192	0.0355
9	1	8	10	8	2	7	9	6441,0192	0.0111
9	1	8	8	8	2	7	7	6441,2301	-0.0360
9	1	8	11	8	2	7	10	6441,446	-0.0009
9	2	8	8	9	1	9	8	6624,8807	0.0119
9	2	8	11	9	1	9	11	6625,1567	-0.0006
9	2	8	9	9	1	9	9	6626,7769	-0.0030
2	2	1	1	1	1	0	2	7693,5176	-0.0021
2	2	1	2	1	1	0	2	7702,7873	-0.0028
2	2	1	1	1	1	0	1	7703,5549	-0.0034
2	2	1	4	1	1	0	3	7705,7867	0.0001
2	2	0	4	1	1	0	3	7707,0219	-0.0047



2	2	1	2	1	1	0	3	7708,4536	0.0017
2	2	1	3	1	1	0	2	7709,4354	-0.0021
2	2	0	3	1	1	0	2	7710,7123	0.0079
2	2	1	2	1	1	0	1	7712,8247	-0.0040
2	2	0	2	1	1	0	1	7714,0765	-0.0001
2	2	1	3	1	1	0	3	7715,0989	-0.0004
2	2	0	3	1	1	0	3	7716,3865	0.0203
2	2	0	1	1	1	1	2	7750,9431	0.0014
2	2	0	1	1	1	1	1	7757,6424	0.0014
2	2	1	2	1	1	1	2	7758,9973	0.0080
2	2	1	4	1	1	1	3	7759,9258	-0.0121
2	2	0	2	1	1	1	2	7760,2378	0.0005
2	2	0	4	1	1	1	3	7761,1771	-0.0009
2	2	0	2	1	1	1	3	7763,8477	-0.0035
2	2	1	3	1	1	1	2	7765,6515	0.0146
2	2	1	2	1	1	1	1	7765,6515	-0.0371
2	2	0	3	1	1	1	2	7766,9017	-0.0019
2	2	0	2	1	1	1	1	7766,9017	-0.0349
2	2	1	3	1	1	1	3	7769,2268	-0.0240
10	11	10	10	9	0	9	9	12385,3622	0.0009
10	11	10	11	9	0	9	10	12385,4689	0.0011
10	11	10	9	9	0	9	8	12385,6887	0.0010
10	11	10	12	9	0	9	11	12385,7959	0.0020
3	3	1	2	2	2	0	2	12486,598	0.0013
3	3	1	2	2	2	1	2	12487,8637	0.0190
9	4	5	11	9	3	6	11	12489,2857	-0.0320
3	3	1	3	2	2	0	3	12491,5315	-0.0018
3	3	0	3	2	2	1	3	12492,8147	-0.0033
5	3	2	4	4	2	3	3	14870,1171	0.0002
5	3	2	7	4	2	3	6	14871,3452	0.0038
5	3	2	5	4	2	3	4	14873,1768	0.0033
5	3	2	6	4	2	3	5	14874,0263	0.0007
5	3	2	5	4	2	3	5	14874,2972	0.0004
7	3	5	9	6	2	4	8	17175,817	0.0607
7	3	5	6	6	2	4	5	17175,2538	-0.0177
7	3	5	8	6	2	4	7	17177,4231	-0.0373
4	4	1	4	3	3	0	4	17254,3031	-0.0047
4	4	1	6	3	3	0	5	17257,4928	-0.0014
4	4	1	3	3	3	0	2	17258,3507	-0.0008
4	4	1	5	3	3	0	4	17258,8822	-0.0029
4	4	1	4	3	3	0	3	17259,7431	-0.0058

^aFrecuencia observada ^b(Frecuencia observada – Frecuencia calculada)

**Table 7.5.** Summary of 35Cl transitions observed for isotopic species of conformer 3.

J'	K ₁ '	K ₊₁ '	F'	J''	K ₁ ''	K ₊₁ ''	F''	obs. ^a	o. - c. ^b
5	1	4	4	5	0	5	4	2276,9301	0.0042
5	1	4	7	5	0	5	7	2281,6314	0.0038
5	1	4	5	5	0	5	5	2293,458	-0.0005
5	1	4	6	5	0	5	6	2298,128	0.0014
4	1	3	4	3	2	2	3	2300,8754	0.0022
4	1	3	5	3	2	2	4	2306,2574	-0.0214
1	1	1	2	0	0	0	2	2451,5239	-0.0003
1	1	1	3	0	0	0	2	2466,2551	0.0022
1	1	1	1	0	0	0	2	2477,747	-0.0045
3	0	3	4	2	1	1	3	2567,0396	-0.0031
1	1	0	1	0	0	0	2	2571,7424	0.0019
3	0	3	3	2	1	1	2	2576,1901	0.0326
1	1	0	3	0	0	0	2	2578,4016	0.0007
3	0	3	5	2	1	1	4	2578,6333	-0.0017
1	1	0	2	0	0	0	2	2587,1617	-0.0039
3	0	3	2	2	1	1	1	2587,4872	0.0088
2	0	2	2	1	0	1	2	2644,2241	-0.0133
2	0	2	3	1	0	1	2	2647,6389	0.0023
2	0	2	4	1	0	1	3	2648,7494	0.0026
5	2	4	6	5	1	4	6	2735,2079	0.0000
5	2	4	5	5	1	4	5	2738,6413	0.0077
3	0	3	4	2	1	2	3	2934,2123	0.0017
6	2	4	7	6	1	5	7	2976,0635	-0.0032
6	2	4	6	6	1	5	6	2976,4006	0.0003
6	2	4	8	6	1	5	8	2977,6213	-0.0001
6	2	4	5	6	1	5	5	2978,0749	-0.0001
4	2	3	4	4	1	3	4	3008,1457	0.0003
7	2	5	6	7	1	6	6	3014,1246	0.0052
7	2	5	9	7	1	6	9	3014,4564	-0.0074
7	2	5	7	7	1	6	7	3015,6497	0.0126
7	2	5	8	7	1	6	8	3015,9112	0.0031
4	2	3	6	4	1	3	6	3017,0006	0.0019
4	2	3	3	4	1	3	3	3021,7547	-0.0038
2	2	0	3	2	1	2	2	3759,2497	0.0053
5	1	4	5	4	2	2	4	3759,4525	-0.0053
2	2	1	2	2	1	2	3	3759,9411	-0.0011
2	2	1	1	2	1	2	2	3760,1705	0.0024
5	1	4	6	4	2	2	5	3761,2602	-0.0012
2	2	0	4	2	1	2	4	3761,6295	-0.0057
2	2	1	4	2	1	2	3	3761,7512	0.0043
2	2	0	2	2	1	2	2	3762,6355	0.0022
2	2	0	3	2	1	2	3	3765,516	0.0021



2	2	0	1	2	1	2	2	3767,5915	-0.0125
2	2	0	2	2	1	2	3	3768,9003	-0.0024
2	2	0	4	2	1	2	3	3770,2882	0.0024
3	1	3	3	2	1	2	2	3804,4493	-0.0034
3	1	3	5	2	1	2	4	3805,8567	0.0022
3	1	3	4	2	1	2	3	3807,4348	0.0309
5	1	4	4	4	2	3	3	3873,3031	-0.0511
7	2	6	9	7	1	7	9	5282,7789	-0.0029
7	2	6	7	7	1	7	7	5291,9413	0.0040
7	2	6	8	7	1	7	8	5294,3174	-0.0003
7	3	5	8	7	2	5	8	5302,7378	-0.0018
7	3	5	7	7	2	5	7	5304,675	-0.0023
4	2	3	3	3	2	2	2	5306,7343	-0.0007
4	2	3	6	3	2	2	5	5307,5925	-0.0056
4	2	3	5	3	2	2	4	5309,6437	-0.0053
4	3	2	6	3	2	2	5	11301,5812	0.0015
4	3	2	3	3	2	2	2	11301,9256	0.0018
4	3	1	5	3	2	2	4	11303,108	0.0002
4	3	1	4	3	2	2	3	11303,6164	0.0005
4	3	1	6	3	2	2	5	11304,2758	0.0024
4	3	1	3	3	2	2	2	11304,5531	0.0008
4	3	1	3	3	2	2	3	11304,7649	0.0001
9	1	9	10	8	0	8	9	11443,7236	0.0023
9	1	9	9	8	0	8	8	11444,0038	0.0054
9	1	9	8	8	0	8	7	11446,4728	0.0012
7	2	6	8	6	1	5	7	11662,0125	-0.0030
7	2	6	7	6	1	5	6	11664,7597	0.0011
7	2	6	9	6	1	5	8	11673,3679	0.0011
5	3	3	7	4	2	2	6	12538,3763	0.0036
5	3	3	4	4	2	2	3	12540,3307	0.0004
5	3	2	6	4	2	2	5	12544,2371	0.0048
5	3	2	5	4	2	2	4	12546,1082	-0.0005
5	3	2	7	4	2	2	6	12549,1064	0.0050
5	3	2	4	4	2	2	3	12550,9655	0.0045
7	2	5	9	6	1	5	8	12587,4961	0.0053
7	2	5	8	6	1	5	7	12587,7089	0.0083
7	2	5	6	6	1	5	5	12587,9858	0.0031
6	2	4	6	5	1	5	5	12968,6501	0.0090
6	2	4	7	5	1	5	6	12973,8164	-0.0092
4	4	1	4	3	3	0	3	13665,9449	0.0083
4	4	0	4	3	3	0	3	13665,9449	-0.0070
5	5	1	7	4	4	1	6	17382,1412	-0.0285
5	5	0	7	4	4	1	6	17382,1412	-0.0291

^aFrecuencia observada ^b(Frecuencia observada – Frecuencia calculada)

**Table 7.6.** Summary of 37Cl transitions observed for isotopic species of conformer 3.

J'	K ₁ '	K ₊₁ '	F'	J''	K ₁ ''	K ₊₁ ''	F''	obs. ^a	o. - c. ^b
1	1	1	2	0	0	0	2	2418,8125	0.0012
1	1	0	3	0	0	0	2	2543,5707	-0.0018
1	1	0	2	0	0	0	2	2550,4287	0.0051
2	0	2	3	1	0	1	2	2613,1527	0.0107
3	0	3	2	2	1	2	1	2882,8944	0.0050
3	0	3	5	2	1	2	4	2888,8301	-0.0005
3	0	3	3	2	1	2	2	2891,9488	0.0027
6	2	4	7	6	1	5	7	2930,6707	0.0080
6	2	4	6	6	1	5	6	2930,9076	0.0120
6	2	4	8	6	1	5	8	2931,7466	0.0047
6	2	4	5	6	1	5	5	2932,0541	0.0008
4	2	3	5	4	1	3	5	2950,7899	-0.0026
3	2	2	4	3	1	2	4	3171,4616	0.0017
3	2	2	3	3	1	2	3	3177,0854	0.0036
3	2	2	5	3	1	2	5	3183,6056	-0.0007
2	2	1	3	2	1	1	3	3338,0167	0.0074
2	2	1	4	2	1	1	3	3342,3897	-0.0375
2	2	1	3	2	1	1	2	3346,1597	0.0062
2	2	0	3	2	1	1	3	3347,4804	0.0011
2	2	1	2	2	1	1	2	3349,1816	-0.0053
2	2	0	2	2	1	1	3	3350,0019	-0.0320
2	2	0	4	2	1	1	3	3351,102	0.0308
2	2	1	4	2	1	1	4	3353,7989	0.0007
2	2	0	3	2	1	1	2	3355,6274	0.0038
2	2	0	2	2	1	1	2	3358,1858	0.0075
2	2	0	4	2	1	1	4	3362,4406	-0.0015
4	0	4	5	3	1	2	4	3589,9361	-0.0043
4	0	4	6	3	1	2	5	3601,461	0.0049
2	1	2	3	1	0	1	2	3613,8914	-0.0009
2	1	2	3	1	0	1	3	3618,4126	-0.0082
2	1	2	2	1	0	1	2	3618,7951	0.0034
2	1	2	4	1	0	1	3	3625,2	-0.0002
2	1	2	2	1	0	1	1	3626,9944	-0.0053
2	1	2	1	1	0	1	1	3633,7279	-0.0039
2	2	1	3	2	1	2	4	3695,2135	-0.0202
4	1	4	6	3	1	3	5	4995,5781	-0.0051
4	0	4	5	3	0	3	4	5160,2384	0.0053
4	0	4	3	3	0	3	3	5160,5116	0.0167
4	0	4	4	3	0	3	3	5161,0455	0.0225
5	0	5	5	4	1	4	4	5700,7675	-0.0010
5	0	5	6	4	1	4	5	5702,5287	0.0396
4	3	2	4	4	2	2	4	5773,6586	-0.0218



4	3	1	5	4	2	2	5	5774,36	-0.0026
4	3	2	6	4	2	2	6	5777,8714	-0.0077
4	3	1	6	4	2	2	6	5780,6847	0.0042
4	3	1	3	4	2	2	3	5782,9311	0.0012
4	3	2	5	4	2	3	5	5901,6778	0.0022
4	3	2	4	4	2	3	4	5902,5868	0.0214
4	3	2	6	4	2	3	6	5904,2072	-0.0021
4	3	1	5	4	2	3	5	5904,6122	0.0036
4	3	1	6	4	2	3	6	5907,0071	-0.0035
4	3	1	3	4	2	3	3	5907,8552	-0.0103
5	3	3	5	5	2	4	5	5948,3641	-0.0005
5	3	3	4	5	2	4	4	5949,0715	0.0065
5	3	2	6	5	2	4	6	5959,6073	-0.0007
5	3	2	7	5	2	4	7	5960,0722	-0.0063
2	2	1	3	1	1	0	2	6080,5412	-0.0003
2	2	1	2	1	1	0	2	6083,5725	-0.0025
2	2	1	3	1	1	0	3	6087,3945	0.0020
2	2	0	3	1	1	0	2	6090,0108	-0.0008
2	2	1	2	1	1	0	3	6090,4214	-0.0045
2	2	1	4	1	1	0	3	6091,813	0.0025
2	2	0	2	1	1	0	2	6092,5612	-0.0050
5	1	5	4	4	1	4	3	6230,3712	0.0028
5	1	5	7	4	1	4	6	6230,7094	-0.0100
5	1	5	6	4	0	4	5	6922,452	-0.0051
5	1	5	6	4	0	4	6	6923,1674	0.0127
5	1	5	5	4	0	4	4	6924,4287	-0.0034
5	1	5	4	4	0	4	3	6931,0515	-0.0030
5	4	1	6	4	3	2	5	14786,0523	-0.0007
5	4	2	5	4	3	2	4	14786,2791	0.0055
5	4	1	5	4	3	2	4	14786,3979	-0.0258
5	4	1	7	4	3	2	6	14787,3497	-0.0050
5	4	1	4	4	3	2	3	14787,5916	0.0220
7	3	4	6	6	2	5	5	15335,1023	-0.0730
7	3	4	7	6	2	5	6	15337,9585	0.0152
7	3	4	8	6	2	5	7	15338,3901	-0.0296
5	5	1	5	4	4	0	4	17132,9137	0.0656
5	5	0	5	4	4	0	4	17132,9137	0.0651
5	5	1	5	4	4	1	4	17132,9137	0.0495
5	5	0	5	4	4	1	4	17132,9137	0.0490
5	5	0	7	4	4	0	6	17133,5986	-0.0336
5	5	0	7	4	4	0	6	17133,5986	-0.0336
5	5	1	7	4	4	1	6	17133,5986	-0.0491
5	5	0	7	4	4	1	6	17133,5986	-0.0496

^aFrecuencia observada ^b(Frecuencia observada – Frecuencia calculada)

**Table 7.7.** $^{13}\text{C}(1)$ transitions observed for isotopic species of conformer 1.

J'	K_{-1}'	K_{+1}'	F'	J''	K_{-1}''	K_{+1}''	F''	obs. ^a	o. - c. ^b
2	1	1	1	1	0	1	1	3860,9651	0.0006
2	1	1	2	1	0	1	2	3863,728	-0.0291
2	1	1	4	1	0	1	3	3866,245	-0.0047
2	1	1	3	1	0	1	2	3874,8039	-0.0076
3	1	2	2	2	0	2	1	5367,7931	-0.0094
3	1	2	5	2	0	2	4	5371,1838	-0.0084
3	1	2	3	2	0	2	2	5378,3736	0.0015
3	1	2	4	2	0	2	3	5381,9372	0.0007
4	1	4	6	3	1	3	5	5553,8386	0.0008
4	1	4	5	3	1	3	4	5554,194	-0.0020
2	2	0	3	1	1	0	2	5637,2789	-0.0257
2	2	0	2	1	1	0	2	5641,6727	-0.0059
4	0	4	6	3	0	3	5	5648,391	-0.0082
2	2	1	4	1	1	0	3	5649,5291	0.0269
2	2	0	4	1	1	0	3	5651,9748	0.0071
2	2	1	4	1	1	1	3	5702,2621	-0.0169
2	2	0	4	1	1	1	3	5704,7439	-0.0006
2	2	1	3	1	1	1	2	5710,8396	0.0007
6	4	2	6	6	3	4	6	6608,3944	-0.0214
4	1	3	3	3	0	3	2	6905,3626	-0.0102
4	1	3	6	3	0	3	5	6909,0903	-0.0094
4	1	3	4	3	0	3	3	6917,4922	-0.0010
4	1	3	5	3	0	3	4	6921,1897	0.0042
3	2	1	4	2	1	1	3	7010,0394	-0.0263
3	2	2	5	2	1	1	4	7011,1312	0.0090
3	2	1	5	2	1	1	4	7023,6315	0.0060
3	2	2	3	2	1	2	4	7177,0076	-0.0032
3	2	2	3	2	1	2	2	7179,3339	-0.0037
3	2	2	4	2	1	2	3	7185,5085	-0.0056
3	2	1	5	2	1	2	4	7189,5063	-0.0031
3	3	0	3	2	2	0	2	8982,0396	-0.0160
3	3	0	4	2	2	0	3	8982,5189	-0.0089
3	3	0	2	2	2	0	1	8984,2216	-0.0017
3	3	0	5	2	2	0	4	8984,7806	0.0026
3	3	1	4	2	2	1	3	8985,6603	0.0273
3	3	1	5	2	2	1	4	8987,1891	0.0146
5	2	3	6	4	1	3	5	9725,5922	-0.0093
5	2	3	5	4	1	3	4	9729,1905	-0.0080
5	2	3	4	4	1	3	3	9737,7765	0.0126
6	1	5	8	5	0	5	7	10102,8147	-0.0109
6	1	5	6	5	0	5	5	10114,0521	0.0043
7	1	7	9	6	0	6	8	10181,6971	-0.0321



7	1	7	6	6	0	6	5	10183,2576	-0.0027
5	2	4	4	4	1	4	3	10209,3407	-0.0028
5	2	4	5	4	1	4	4	10219,6191	0.0026
5	2	4	6	4	1	4	5	10223,0236	-0.0013
4	3	1	5	3	2	1	4	10394,706	-0.0123
4	3	1	4	3	2	1	3	10396,2468	-0.0132
7	6	2	6	7	5	2	7	10398,4094	-0.0225
4	3	1	3	3	2	1	2	10399,8346	0.0134
6	2	4	7	5	1	4	6	11088,7534	-0.0117
6	2	4	8	5	1	4	7	11094,6478	0.0076
6	2	4	5	5	1	4	4	11097,1343	0.0066
7	1	6	9	6	0	6	8	11769,378	-0.0023
6	2	5	8	5	1	5	7	11773,5462	-0.0088
6	2	5	6	5	1	5	5	11781,482	-0.0042
6	2	5	7	5	1	5	6	11784,3816	-0.0060
7	1	6	8	6	0	6	7	11785,1603	-0.0007
5	3	3	6	4	2	3	5	11837,5329	-0.0058
6	3	4	7	5	2	4	6	13274,5716	-0.0029
6	3	4	5	5	2	4	4	13275,0015	0.0066
8	2	6	8	7	1	6	7	13881,6413	0.0125
7	3	5	6	6	2	5	5	14721,7718	0.0032
7	3	5	9	6	2	5	8	14721,7718	0.0003
7	3	5	8	6	2	5	7	14722,432	0.0036
7	3	5	7	6	2	5	6	14722,432	0.0009
6	4	2	8	5	3	2	7	15131,5098	0.0352
6	4	3	8	5	3	3	7	15133,4334	0.0446

^aFrecuencia observada ^b(Frecuencia observada – Frecuencia calculada)

**Table 7.8.** $^{13}\text{C}(2)$ transitions observed for isotopic species of conformer 1.

J'	K ₁ '	K ₊₁ '	F'	J''	K ₁ ''	K ₊₁ ''	F''	obs. ^a	o. - c. ^b
2	1	1	2	1	0	1	2	3869,8921	-0.0049
2	1	1	4	1	0	1	3	3872,3768	-0.0124
2	1	1	3	1	0	1	2	3880,9577	0.0065
2	1	1	2	1	0	1	1	3882,3775	0.0017
3	1	2	2	2	0	2	1	5379,1884	-0.0306
3	1	2	2	2	0	2	1	5379,1884	-0.0306
3	1	2	5	2	0	2	4	5382,5997	-0.0121
3	1	2	3	2	0	2	2	5389,7922	-0.0002
2	2	1	4	1	1	0	3	5647,0321	-0.0063
3	2	1	3	2	1	1	2	7022,6874	-0.0035
3	2	1	3	2	1	1	2	7022,6874	-0.0035
3	2	1	5	2	1	1	4	7026,0758	-0.0002
5	1	5	6	4	0	4	5	7641,1074	-0.0259
5	1	5	5	4	0	4	4	7644,2957	-0.0081
5	1	5	7	4	0	4	6	7651,4645	0.0086
3	3	1	4	2	2	1	3	8980,028	-0.0180
3	3	1	4	2	2	1	3	8980,028	-0.0180
3	3	1	2	2	2	1	1	8980,4822	-0.0111
3	3	1	2	2	2	1	1	8980,4822	-0.0111
3	3	1	5	2	2	1	4	8981,571	-0.0138
5	2	3	6	4	1	3	5	9738,1455	-0.0197
5	2	3	7	4	1	3	6	9746,6849	0.0024
5	2	3	4	4	1	3	3	9750,2919	0.0126
6	1	5	5	5	0	5	4	10127,7341	-0.0256
6	1	5	5	5	0	5	4	10127,7341	-0.0256
6	1	5	6	5	0	5	5	10142,3619	0.0108
6	1	5	7	5	0	5	6	10145,777	0.0200
5	2	4	4	4	1	4	3	10222,8499	-0.0213
5	2	4	4	4	1	4	3	10222,8499	-0.0213
5	2	4	7	4	1	4	6	10226,2079	-0.0148
5	2	4	5	4	1	4	4	10233,1495	0.0045
5	2	4	6	4	1	4	5	10236,5644	0.0107
4	3	2	6	3	2	1	5	10393,5476	0.0025
4	3	2	5	3	2	1	4	10393,8754	-0.0260
4	3	2	4	3	2	1	3	10395,9803	-0.0354
4	3	1	6	3	2	1	5	10397,6397	-0.0105
4	3	2	3	3	2	1	2	10398,6662	0.0178
4	3	2	6	3	2	2	5	10406,191	0.0008
4	3	1	6	3	2	2	5	10410,2776	-0.0178

^aFrecuencia observada ^b(Frecuencia observada – Frecuencia calculada)

**Table 7.9.** $^{13}\text{C}(3)$ transitions observed for isotopic species of conformer 1.

J'	K ₁ '	K ₊₁ '	F'	J''	K ₁ ''	K ₊₁ ''	F''	obs. ^a	o. - c. ^b
2	1	1	1	1	0	1	1	3857,6391	-0.0001
2	1	1	2	1	0	1	2	3860,4187	-0.0124
2	1	1	4	1	0	1	3	3862,9176	-0.0064
2	1	1	3	1	0	1	3	3878,367	0.0093
3	1	2	5	2	1	1	4	4331,1302	0.0000
3	1	2	4	2	1	1	3	4332,6302	0.0020
3	1	3	4	2	0	2	3	5016,5132	-0.0188
3	1	3	5	2	0	2	4	5029,6506	-0.0067
3	1	2	2	2	0	2	2	5355,2262	-0.0095
3	1	2	2	2	0	2	1	5361,4863	0.0037
3	1	2	4	2	0	2	3	5375,6059	-0.0027
3	1	2	4	2	0	2	4	5381,8085	0.0083
2	2	1	2	1	1	1	1	5689,4019	-0.0188
2	2	1	4	1	1	1	3	5703,4708	-0.0362
2	2	1	3	1	1	1	2	5712,0615	-0.0066
4	1	3	3	3	0	3	2	6895,8129	0.0001
4	1	3	6	3	0	3	5	6899,5318	-0.0060
4	1	3	4	3	0	3	3	6907,9217	-0.0037
3	2	2	4	2	1	1	3	6995,2515	-0.0171
3	2	1	3	2	1	1	3	7008,4992	-0.0112
3	2	2	5	2	1	1	4	7010,6474	-0.0041
3	2	1	3	2	1	1	2	7019,554	-0.0111
3	2	1	5	2	1	1	4	7022,9627	-0.0033
3	2	2	5	2	1	2	4	7175,4303	-0.0038
3	2	2	3	2	1	2	2	7177,7599	-0.0052
3	2	2	2	2	1	2	2	7177,8441	-0.0028
3	2	2	4	2	1	2	3	7183,9312	-0.0111
3	2	1	5	2	1	2	4	7187,7496	0.0010
3	2	1	4	2	1	2	3	7198,0463	-0.0178
4	2	3	6	3	1	2	5	8340,7518	0.0066
4	2	3	3	3	1	2	2	8347,7574	0.0304
4	2	3	6	3	1	3	5	8675,9554	-0.0009
4	2	3	4	3	1	3	3	8681,3087	-0.0021
4	2	3	5	3	1	3	4	8685,5369	-0.0058
5	2	3	6	4	1	3	5	9720,2155	-0.0066
5	2	3	5	4	1	3	4	9723,8342	0.0029
5	2	3	7	4	1	3	6	9728,8247	0.0065
6	1	5	5	5	0	5	4	10082,4693	-0.0085
6	1	5	8	5	0	5	7	10085,8163	-0.0025
6	1	5	6	5	0	5	5	10097,0273	0.0015
6	1	5	7	5	0	5	6	10100,416	-0.0028
5	2	4	4	4	1	4	3	10201,6494	0.0110



5	2	4	7	4	1	4	6	10204,9939	0.0051
5	2	4	5	4	1	4	4	10211,9149	0.0044
5	2	4	6	4	1	4	5	10215,3206	0.0020
4	3	2	5	3	2	1	4	10394,9749	-0.0336
4	3	1	5	3	2	1	4	10395,5232	-0.0191
4	3	1	4	3	2	1	3	10397,0655	-0.0028
4	3	1	6	3	2	1	5	10399,1964	-0.0105
4	3	1	3	3	2	1	2	10400,6278	-0.0028
4	3	2	4	3	2	2	3	10409,9664	-0.0003
6	2	4	7	5	1	4	6	11080,5506	-0.0128
6	2	4	8	5	1	4	7	11086,5798	0.0049
7	1	6	9	6	0	6	8	11748,081	0.0040
7	1	6	7	6	0	6	6	11760,5976	-0.0039
6	2	5	6	5	1	5	5	11770,4669	0.0177
6	2	5	7	5	1	5	6	11773,3539	0.0040
5	3	2	6	4	2	2	5	11797,2271	0.0003
5	3	2	5	4	2	2	4	11798,7399	0.0062
5	3	2	7	4	2	2	6	11801,3717	0.0368
5	3	3	6	4	2	3	5	11835,6017	0.0127
5	3	3	5	4	2	3	4	11836,0765	0.0096
5	3	3	7	4	2	3	6	11836,691	0.0043
5	3	2	5	4	2	3	5	11837,1807	0.0214
5	3	2	4	4	2	3	3	11839,1243	0.0186
6	3	4	7	5	2	4	6	13269,9394	0.0077
6	3	4	8	5	2	4	7	13270,1445	-0.0078
6	3	4	5	5	2	4	4	13270,3865	0.0203
5	4	1	7	4	3	1	6	13716,6187	0.0319
5	4	2	7	4	3	2	6	13716,9657	0.0216

^aFrecuencia observada ^b(Frecuencia observada – Frecuencia calculada)
